

Energy Advances

Accepted Manuscript

This article can be cited before page numbers have been issued, to do this please use: S. Y. Kim, N. Rayes, A. Kemanian, E. D. Gomez and N. Y. Doumon, *Energy Adv.*, 2024, DOI: 10.1039/D4YA00492B.



This is an Accepted Manuscript, which has been through the Royal Society of Chemistry peer review process and has been accepted for publication.

Accepted Manuscripts are published online shortly after acceptance, before technical editing, formatting and proof reading. Using this free service, authors can make their results available to the community, in citable form, before we publish the edited article. We will replace this Accepted Manuscript with the edited and formatted Advance Article as soon as it is available.

You can find more information about Accepted Manuscripts in the [Information for Authors](#).

Please note that technical editing may introduce minor changes to the text and/or graphics, which may alter content. The journal's standard [Terms & Conditions](#) and the [Ethical guidelines](#) still apply. In no event shall the Royal Society of Chemistry be held responsible for any errors or omissions in this Accepted Manuscript or any consequences arising from the use of any information it contains.

Semitransparent Organic and Perovskite Photovoltaics for Agrivoltaic Applications

Souk Y. Kim,^{1§} Noura Rayes,^{1§} Armen R. Kemanian,² Enrique D. Gomez,^{1,3,4} and Nutifafa Y. Doumon^{*1,4,5}

¹Department of Materials Science and Engineering, The Pennsylvania State University, University Park, PA 16802, United States

²Department of Plant Science, The Pennsylvania State University, University Park, PA 16802, United States

³Department of Chemical Engineering, The Pennsylvania State University, University Park, PA 16802

⁴Materials Research Institute, The Pennsylvania State University, University Park, Pennsylvania 16802, United States

⁵Department of Engineering Science and Mechanics, The Pennsylvania State University, University Park, PA, 16802 USA

§ These authors contributed equally to the manuscript

*Corresponding author: nzd5349@psu.edu

Abstract:

Greenhouse structures offer the ability to control the microclimate of plants, enabling year-round crop cultivation and precision agriculture techniques. To maintain optimal crop growth conditions, substantial energy is required to heat, light, irrigate, and ventilate the interior greenhouse environment. The term *Agrivoltaics* is coined from integrating agricultural land management with renewable solar energy systems. Most agrivoltaic research applications have focused on studying opaque silicon photovoltaics, with limited exploration of novel semitransparent photovoltaics such as organic or perovskite photovoltaics. By incorporating semitransparent photovoltaic systems onto greenhouse rooftops, farms can partially generate electricity from solar energy while utilizing the remaining rooftop light transmission to nurture greenhouse plant growth below. This review explores the principles and properties of semitransparent organic and perovskite photovoltaic technologies and their potential benefits for greenhouse applications. Additionally, we discuss practical case studies to illustrate their integration and efficacy in agrivoltaic systems. We also address key metrics such as average visible transmittance, average photosynthetic transmittance, light utilization efficiency, power conversion efficiency, and their impact on greenhouse energy production. We conclude with an analysis of device challenges, including stability and toxicity issues, limited experimental results of semitransparent photovoltaics in current greenhouse agrivoltaics, and the prospects for integrating ST-OPVs and ST-PPVs into agrivoltaic systems.

Keywords: Organic photovoltaics, Perovskite photovoltaics, Greenhouse, Semitransparent photovoltaics, and Agrivoltaics.

Acronyms:

OPVs	Organic photovoltaics
PPVs	Perovskite photovoltaics
ST-PVs	Semitransparent photovoltaics
AVT	Average visible transmittance
LUE	Light utilization efficiency (LUE = Device Power Conversion Efficiency (PCE) × AVT)



1. Background

Sustainable energy development is crucial for addressing the challenges posed by climate change. The accelerated pace of environmental degradation is primarily attributed to land exploitation to expand agricultural and energy infrastructures needed to support our growing population.¹ Hunter et al. predict that a 25-70% increase above current production levels will be necessary by 2050 to meet food demand projections.² To sustain this growth rate without exacerbating ecological harm, farmers and engineers must find ways to optimize the efficiency of existing agricultural land. The strain imposed on our natural environment has already contributed to alarming ecological predictions: a 23% loss of wildlife habitat by the end of the century and a 69% decline in biodiversity since 1970.³⁻⁵

The food, water, and energy nexus pertains to how communities can balance the demand for natural resources to sustain human health and environmental integrity across the world. Agriculture, which accounts for 72% of all freshwater withdrawals and 10.6% of total U.S. emissions since 2021, is at the core of this challenge.^{6,7} However, agrivoltaic systems—combining agriculture and solar energy—offer a promising solution for communities to sustainably support these needs. Engineers and farmers must advocate for sustainable agricultural policies to support the research and development of novel precision farming technologies. In this review, we discuss solutions to this grand challenge that utilize the unique properties of innovative photovoltaic technologies.

Introduction to Agrivoltaics

Agrivoltaics describes the integration of photovoltaic (PV) systems with agriculture to optimize land for both energy production and farming practices.^{8,9} Agrivoltaic techniques have also been applied in industrial greenhouses to reduce existing energy demands for farmers, thereby promoting economic and environmental sustainability.⁹ The primary aim of greenhouses is to maintain a controlled microenvironment favorable to the year-round cultivation of produce. In terms of energy consumption, greenhouses use passive solar to reduce heating costs; however, energy savings can reach up to 80% through further retrofit of conventional design.¹⁰ In particular, electricity for these structures can be generated on-site by partially incorporating PV modules into the rooftop infrastructure, further conserving more land space. **Figure 1a** highlights the general principle for land use efficiency of these systems. **Figure 1b** is a representative model for semitransparent photovoltaics (ST-PVs) integration with greenhouses, modified from Macknick et al., while **Figures 1c** and **d** demonstrate real-life implementations of this concept.^{8,11,12}

Typically, greenhouses are constructed with a metallic framework and covered with durable transparent materials, such as plastic or glass, to protect crops against severe weather conditions.¹³ Various designs have been explored for integrating PV modules into greenhouses using partial shading and transparency techniques to provide a plant species with the select wavelengths that may be necessary for optimal growth.¹⁴ Luminescent solar concentrators propagate light from the sun via a waveguide to photovoltaic cells and have exhibited similar partial shading and energy harvesting properties fitting for these exact systems.¹⁵⁻¹⁸ More ST-PV



technologies are increasing in scalability, efficiency, and longevity.¹⁶ Due to their selective light absorption properties and higher efficiencies, ST-PVs are a competitive alternative to standard greenhouse solar energy generation in the future.^{14,19}

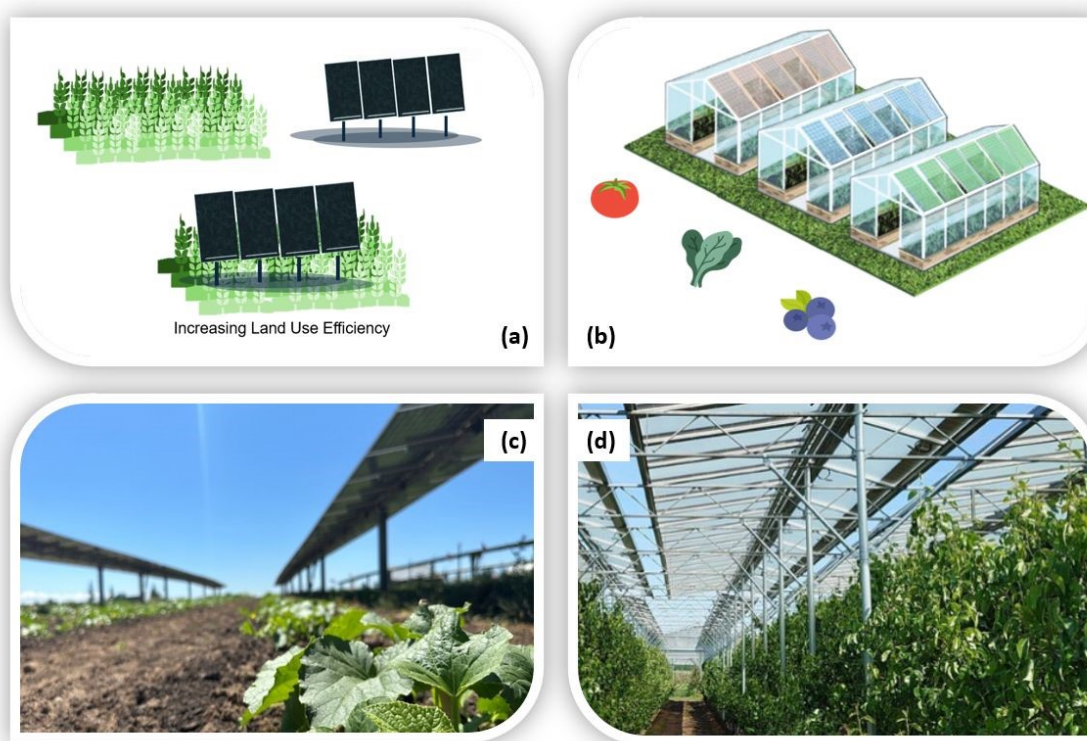


Figure 1. (a) Visual concept of agrivoltaic dual land use efficiency. (b) The visual concept of ST-OPVs for potential greenhouse applications. Reproduced with permission.⁸ Copyright NREL (c) Crops grown under solar panels at Oregon State University. Reproduced with permission.¹¹ Copyright USDA (d) OPV panels on top of a greenhouse installation at Brite Solar Nanomaterials. Reproduced with permission.¹² Copyright Brite Solar.

1.1 Technology Principles

Traditional greenhouse agrivoltaics often utilize opaque crystalline silicon and thin-film PVs attached to the roof, which can decrease crop yields due to increased shading.²⁰ To increase transmission, transparent and translucent photovoltaics have been explored. Transparent devices allow light to pass through them without scattering, while translucent devices refer to semitransparent devices that scatter the incoming light. Organic photovoltaics (OPVs) and perovskite photovoltaics (PPVs) are promising alternatives in solar energy harvesting and agrivoltaic applications because of their semitransparent properties. In principle, PVs convert light into electrical energy using semiconducting materials sandwiched between two electrodes. The semiconductor in the photoactive layer is designed with an appropriate energy bandgap to absorb the radiation of the sun with high efficiency. Photons higher in energy than the material's bandgap can be absorbed, creating an electron-hole pair that can then be separated and extracted by the electrodes to generate electricity.²¹ Therefore, lower bandgap semiconductor



materials may absorb a broader range of solar radiation, which is advantageous for maximizing light absorption at the expense of lower produced voltage and increased recombination losses.

OPVs and PPVs are particularly beneficial in agrivoltaic systems due to their selective energy bandgap, which enables the tunability of light absorption. By adjusting the photoactive molecules in OPVs or the composition of PPVs, these devices can be designed to selectively absorb certain regions of the solar spectrum while transmitting wavelengths necessary for plant growth.²² Additionally, both OPVs and PPVs can be produced as flexible panels, allowing easy integration into various greenhouse structures. Despite these similarities, OPVs and PPVs differ in several key aspects, particularly regarding their photoactive constituents. OPVs are based on organic photoactive materials, including small molecules and polymers.^{20,22–27} These materials offer flexibility in molecular design, enabling a wide range of absorption profiles.^{23,24,28,29} PPVs, on the other hand, are composed of perovskite photoactive materials with a unique crystal structure characterized by the formula ABX_3 , where A is a cation (e.g., methylammonium, formamidinium), B is a metal cation (e.g., lead, tin), and X is a halide anion (e.g., iodide, bromide). This versatility in composition contributes to the PPVs' capture of solar energy with high efficiency.³⁰ The detailed properties and applications of these technologies will be discussed in the following sections.

Research efforts have recently pushed efficiencies at 20% for OPVs^{31–33} and over 26% for PPVs.^{34,35} The rapid enhancement of their efficiencies makes OPVs and PPVs with absorption tunability and semi-transparency increasingly attractive for integration into agricultural applications. Additionally, the relative ease and low cost of manufacturing these materials further emphasize their potential for widespread use in agrivoltaics. While studies and review papers discuss semitransparent OPVs and PPVs^{26,27,36–39}, a comprehensive discussion focusing on their applications in agrivoltaics is still key to their advancement. The review examines the progress, challenges, and future of ST-OPVs and ST-PPVs for agrivoltaic applications. We seek to highlight the potential of the latest research and technological breakthroughs to ensure a sustainable agricultural future where energy generation and food production can coexist in synergy.

2. Special Requirements

In agrivoltaics, evaluating the compatibility of ST-PVs alongside agricultural productivity is important in determining the land-use efficiency of the entire system. Therefore, understanding a comprehensive set of figures and metrics from these disciplines is essential to effectively quantifying the relationship between ST-PV and crop yield. The foundation of this work relies on the sun's radiation at Earth's terrestrial surface. After passing through the atmosphere, the total radiation consists of roughly 5% UV, 43% visible, and 52% infrared radiation.⁴⁰ On clear days in the summer, the incoming irradiance at noon at sea level is approximately $1000 \text{ W}\cdot\text{m}^{-2}$. **Figure 2a** illustrates the radiation emitted from the sun in $\text{W}\cdot\text{m}^{-2}\cdot\text{nm}^{-1}$ from 0 to 4000 nm, illustrating the solar irradiance spectra at Earth's atmosphere (AM0) and Earth's surface (AM1.5), respectively. **Figure 2b** depicts which wavelengths of light various bodies, including chlorophyll, phytochromes, and many other plant pigments, will absorb for spectral reference. Solar energy harvesting devices are designed to maximize the energy they can produce through the absorption of solar radiation. Thus, **Figure 2c** shows a typical absorption profile for ST-OPV for the AM 1.5G solar



emission for a potential agrivoltaic system, i.e., ST-PPVs mostly absorb in the UV and NIR while remaining transparent in the visible.

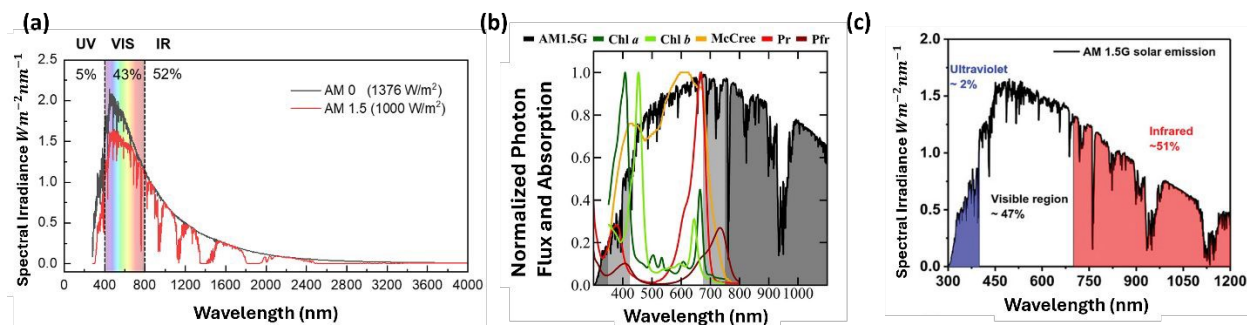


Figure 2. (a) Solar irradiance spectra ($\text{W}/\text{m}^2\text{nm}$) at Earth's atmosphere (AM0) and Earth's surface (AM1.5). The total spectrum is roughly 5% UV, 43% visible, and 52% infrared light. (b) Normalized photon flux and absorption spectra of chlorophyll (Chl) a and b, red-absorbing phytochrome (Pr), far-red-absorbing phytochrome (Pfr), and averaged quantum yield of many plants denoted as McCree. Reproduced with permission.⁴¹ Copyright 2023, Scientific Reports. (c) The absorption spectrum shows the approximate UV and IR regions where an ideal agrivoltaic ST-PPV active layer absorbs light, and the visible region is where they can be transparent. Reproduced with permission.⁴² Copyright 2021, Wiley-VCH GmbH.

Sunlight absorption in plants is necessary for photosynthesis, in which plants utilize light to store chemical energy.⁴³ However, under full sun, most of the energy absorbed by the leaves is dissipated as latent and sensible heat and thermal radiation. Near-infrared is not used for photosynthesis. Similarly, plants reflect most green light and thus present a gap in the visible absorption spectrum in the green. Selective wavelength transmission through the device must be considered when pairing the necessary PV with the desired crop to maximize production yields. Visible light is 43% of the total irradiance at Earth's surface, divided into blue light (400-500 nm), green light (500-600 nm), and red light (600-700 nm).^{41,44} The light absorption spectrum unique to each plant species is known as photosynthetic active radiation, between 400 and 800 nm, shown in **Figure 2**. Various pigments, however, such as chlorophyll A and B within the chloroplast, absorb light wavelengths selectively, thus influencing plant development, leaf area expansion, stem length, and flowering rate.^{41,45} More physiological research is needed to collect photosynthetic active region data for specific greenhouse crops.

The average visible transmittance (AVT), the visible light able to pass through a device, can be derived by averaging the total light transmittance measured from 400 to 800 nm against the photopic response of the human eye.⁴⁶ This metric facilitates comparing device efficiency with light transparency. The light utilization efficiency ($\text{LUE} = \text{PCE} \times \text{AVT}$) can be calculated to further evaluate the performance of ST-PVs.⁴⁷ It is worth noting that LUE in this context is different from light use efficiency, which refers to the efficiency of converting absorbed light into biomass. Unlike AVT, which considers how much incident photon flux passes through a panel, Stallknecht et al. introduced another metric, the average photosynthetic transmittance, which considers the required wavelengths for the specific plant.⁴¹ The average photosynthetic transmittance (APT) replaces photopic response with the relative quantum efficiency of plants averaged among 22 varieties established by McCree et al.⁴⁸ The equation for APT is given by the following:



$$APT = \frac{\int T(\lambda)S(\lambda)P(\lambda)d\lambda}{\int S(\lambda)P(\lambda)d\lambda},$$

where $S(\lambda)$ is the AM 1.5 photon flux, $T(\lambda)$ is the photon transmittance of the device, and $P(\lambda)$ is the average photosynthetic quantum yield.⁴¹ Plant growth efficiency, quality, and yield are vital agricultural benchmarks, directly correlating the system design and operation with agronomic outcomes. Here, we explore these figures of merit, examining how they are used to balance energy production with agricultural productivity to define the success of agrivoltaics systems.

3. Semitransparent Photovoltaics (ST-PVs)

ST-PVs represent a cutting-edge approach to integrating solar energy generation with visual or aesthetic applications, such as building-integrated photovoltaics or agrivoltaics.^{47,49,50} These systems strike a balance between optimal light transmission for underlying plant growth and power generation. We explore two prominent types of ST-PVs: semitransparent organic photovoltaics (ST-OPVs) and perovskite photovoltaics (ST-PPVs). Each system has advantages and challenges in terms of efficiency, transparency, and suitability for agrivoltaic systems.

3.1 ST-OPVs

OPVs have several advantages compared to conventional inorganic solar cells.^{51,52} OPVs can be lightweight, flexible, and semitransparent, utilizing the conjugated structure of organic donor and acceptor molecules to facilitate electron transfer. Furthermore, OPVs can be fabricated using roll-to-roll or slot-die coating, potentially leading to lower industrial costs and utilizing environmentally benign solution processing.^{53,54} However, work is still necessary to improve the efficiency of these devices to match that of inorganic cells. The current efficiency for OPVs has surpassed 20%.^{31,32} Nevertheless, this efficiency is not yet on par with that of their inorganic silicon counterpart, which stands at 26.6%.^{55,56} OPVs are prone to efficiency losses due to the weak intermolecular coupling and the low dielectric constants of the organic donor and acceptor molecules.⁵⁷ The bulk heterojunction morphology is now the most extensively explored active layer structure in these devices to overcome the electron-hole recombination challenges from the bilayer heterojunction cell structure. The bulk heterojunction comprises intricate electron donor and acceptor materials that facilitate exciton diffusion and charge transfer to the corresponding electrodes.⁵⁸ This review explores how previously studied average visible transmittance (AVT) of donor-acceptor materials can be utilized for precision agriculture. For enhanced perspective, the AVT of common glass windows is greater than 25%.⁵⁹ For various active layer blends and thicknesses, the AVT value will change and affect the amount of crop shading and yield.

Initially, a well-studied combination of donor and acceptor materials in OPV systems included P3HT and PCBM molecules (the full names of all organic materials are provided in **Table 1**), as seen in **Figure 3**. However, device performance using PCBM, fullerene molecules, is limited by the weak absorption in the visible and infrared wavelength range.⁶⁰ Even after improving the optimal fabrication parameters for these devices, a limited device efficiency of only 5% was reported in 2005.²² The PCE has improved to 9.35% with the introduction of low-bandgap donor material, PTB7-Th in 2013.⁶¹ The infrared profile of the solar spectrum consists of 52% of the



total irradiance, prompting the investigation of near-infrared acceptors for solar energy harvesting devices.²² In 2015, Zhan et al. reported a novel near-infrared acceptor, ITIC, with the efficiency of blends reported to be 6.8%, and further studies demonstrated the potential for these devices to reach 11.4%.⁶² However, the AVT of solar cells plays an important role in greenhouse systems and is dependent on active layer thickness. When the thickness of the active layer increases, the device absorption will increase, such that the efficiency will rise until the series resistance and recombination rate is too high. In contrast and in agreement with the Beer-Lambert law, AVT decreases with increasing device thickness, as demonstrated in **Figure 4**.

Table 1: Full name of most organic molecules discussed in the review

P3HT	Poly(3-hexylthiophene-2,5-diyl)
PEDOT:PSS	Poly(3,4-ethylenedioxythiophene)-poly(styrenesulfonate)
PC ₆₁ BM	[6,6]-phenyl-C61-butyric acid methyl ester
PC ₇₁ BM	[6,6]-Phenyl C71 butyric acid methyl ester
ITIC	3,9-bis(2-methylene-(3-(1,1-dicyanomethylene)-indanone))-5,5,11,11-tetrakis(4-hexylphenyl)
Y6	2,2'-((2Z,2'Z)-((12,13-bis(2-ethylhexyl)-3,9-diundecyl-12,13-dihydro-[1,2,5]thiadiazolo[3,4-e]thieno[2'',3'':4',5']thieno[2',3':4,5]pyrrolo[3,2-g]thieno[2',3':4,5]thieno[3,2-b]indole-2,10-diyl)bis(methanylylidene))bis(5,6-difluoro-3-oxo-2,3-dihydro-1H-indene-2,1-diylidene))dimalononitrile
PM6	Poly[(2,6-(4,8-bis(5-(2-ethylhexyl-3-fluoro)thiophen-2-yl)-benzo[1,2-b:4,5-b']dithiophene))-alt-(5,5-(1',3'-di-2-thienyl-5',7'-bis(2-ethylhexyl)benzo[1',2'-c:4',5'-c']dithiophene-4,8-dione)]
PBDB-T	Poly[(2,6-(4,8-bis(5-(2-ethylhexyl)thiophen-2-yl)-benzo[1,2-b:4,5-b']dithiophene))-alt-(5,5-(1',3'-di-2-thienyl-5',7'-bis(2-ethylhexyl)benzo[1',2'-c:4',5'-c']dithiophene-4,8-dione)]
Y6-BO	2,2'-((2Z, 2'Z)-((12,13-bis(2-butylloctyl)-3,9-diundecyl-12,13-dihydro-[1,2,5]thiadiazolo[3,4-e]thieno[2'',3 ''':4',5']thieno[2',3':4,5]pyrrolo[3,2-g]thieno[2',3':4,5]thieno[3,2-b]indole-2,10-diyl)bis(methanylylidene))bis(5,6-difluoro-3-oxo-2,3-dihydro-1H-indene-2,1-diylidene))dimalononitrile
2PACz	2-(9H-carbazol-9-yl)ethyl]phosphonic acid
BFN	1,3,5-tri(<i>N</i> -(naphthalene-1-yl)- <i>N'</i> -(1,1'-biphenyl-3-yl)-9,9'-dihexyl-2 <i>H</i> -fluorene-2-yl-amine)benzene
BFSN	1,3,5-tri(<i>N</i> -(naphthalene-1-yl)- <i>N'</i> -(dibenzothiophene-4-yl)-9,9'-2 <i>H</i> -dihexylfluorene-2-yl-amine)benzene
BCP	2,9-Dimethyl-4,7-diphenyl-1,10-phenanthroline
P3HT	Poly(3-hexylthiophene-2,5-diyl)
PDBTT-DPP	Poly{2,6'-4,8-di(5-ethylhexylthienyl)benzo[1,2-b;3,4-b]dithiophene-alt-5,5'-dibutylloctyl-3,6-bis(5-thiophen-2-yl)pyrrolo[3,4-c]pyrrole-1,4-dione}
PBDTT-SeDPP	poly{2,6'-4,8-di(5-ethylhexylthienyl)benzo[1,2-b;3,4-b]dithiophene-alt-2,5-bis(2-butylloctyl)-3,6-bis(selenophene-2-yl)pyrrolo[3,4-c]pyrrole-1,4-dione}
IEIC	2,2'-[[6,6,12,12-Tetrakis(4-hexylphenyl)-6,12-dihydrodithieno[2',3':4,5]-s-indaceno[1,2-b:5,6-b']dithiophene-2,8-diyl]bis[methylidyne(3-oxo-1H-indene-2,1(3H)-diylidene)]]bis[propanedinitrile]
IEICO	2,2'-((2Z,2'Z)-((5,5'-bis(4,4,9,9-tetrakis(4-hexylphenyl)-4,9-dihydro-s-indaceno[1,2-b:5,6-b']dithiophene-2,7-diyl)bis(4-((2-ethylhexyl)oxy)thiophene-5,2-diyl))bis(methanylylidene))bis(3-oxo-2,3-dihydro-1H-indene-2,1-diylidene))dimalononitrile, 2,2'-[[4,4,9,9-tetrakis(4-hexylphenyl)-4,9-dihydro-s-indaceno[1,2-b:5,6-b']dithiophene-2,7-diyl]bis[[4-((2-ethylhexyl)oxy)-5,2-thiophenediyl]-(Z)-methylidyne(3-oxo-1H-indene-2,1(3H)-diylidene)]]bis-propanedinitrile
IEICO-4F	2,2'-((2Z,2'Z)-(((4,4,9,9-tetrakis(4-hexylphenyl)-4,9-dihydro-s-indaceno[1,2-b:5,6-b']dithiophene-2,7-diyl)bis(4-((2-ethylhexyl)oxy)thiophene-5,2-diyl))bis(methanylylidene))bis(5,6-difluoro-3-oxo-2,3-dihydro-1H-indene-2,1-diylidene))dimalononitrile



PTB7	Poly [[4,8-bis(2-ethylhexyl)oxy]benzo[1,2-b:4,5-b']dithiophene-2,6-diyl][3-fluoro-2-[(2-ethylhexyl)carbonyl]thieno[3,4-b]thiophenediyl]]
PBDTTT-C	Poly[(4,8-bis(2-ethylhexyloxy)benzo[1,2-b:4,5-b']dithiophene-2,6-diyl)-alt-(4-(2-ethylhexyl)-3-fluorothieno[3,4-b]thiophene-)-2-carboxylate-2,6-diyl)]
ITCC	3,9-bis(2-methylene-((3-(1,1-dicyanomethylene)-5,6-difluoro-1H-indene-1,2(3H)-diylidene)))5,5,11,11-tetrakis(4-hexylphenyl)-dithieno[2,3-d:2',3'-d']-s-indaceno[1,2-b:5,6-b']dithiophene
IT-M	3,9-bis(2-methylene-((3-(1,1-dicyanomethylene)-6/7-methyl)-indanone))-5,5,11,11-tetrakis(4-hexylphenyl)-dithieno[2,3-d:2',3'-d']-s-indaceno[1,2-b:5,6-b']dithiophene
IT-4F	3,9-bis(2-methylene-((3-(1,1-dicyanomethylene)-6,7-difluoro)-indanone))-5,5,11,11-tetrakis(4-hexylphenyl)-dithieno[2,3-d:2',3'-d']-s-indaceno[1,2-b:5,6-b']dithiophene

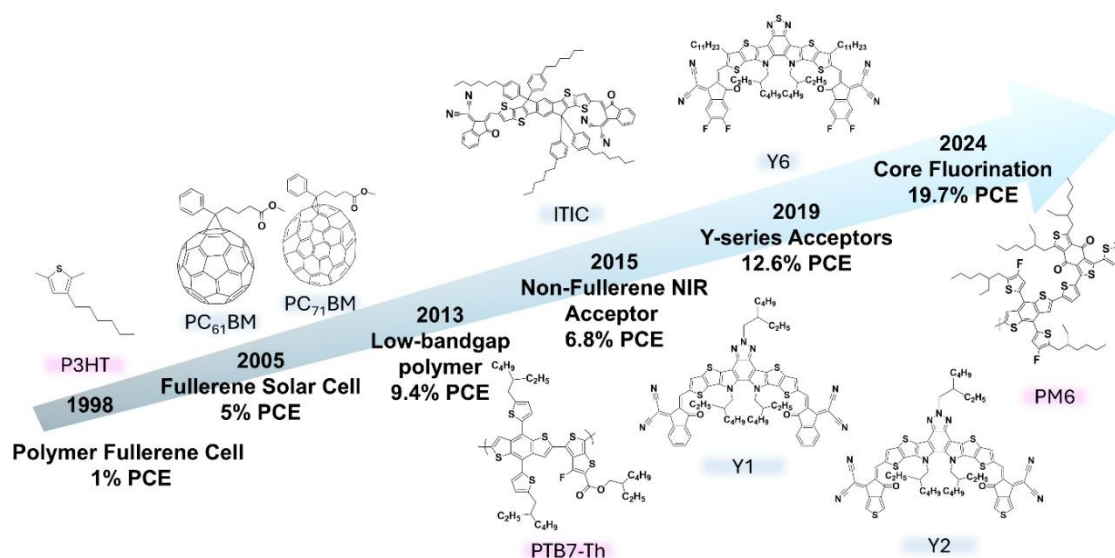


Figure 3. Timeline of selected donor (pink highlight) and acceptor (blue highlight) workhorse materials discussed in this paper for OPV systems from 1998 to 2024. ^{22,62–64}

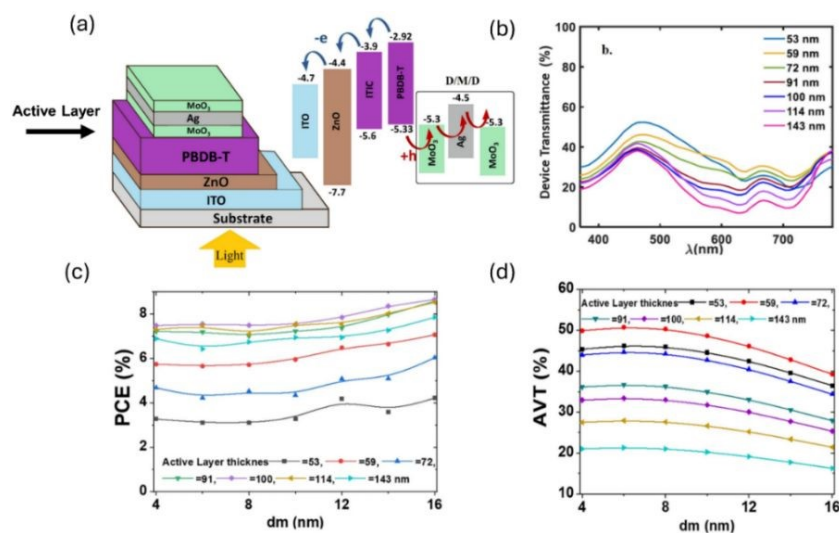


Figure 4. (a) Device structure and OPV band diagram of ITO/ZnO/PBDB-T:ITIC/MoO₃/Ag/MoO₃. (b) Device transmittance over the visible spectra with varying active layer thickness of $t = 53, 59, 72, 91, 100, 114, 143$ nm. (c) Power conversion efficiency of various active layer thicknesses relative to varying Ag cathode thicknesses. (d) AVT



over the range of active layer thicknesses relative to varying Ag cathode thicknesses. Reproduced with permission.⁵⁹ Copyright 2022, Scientific Reports.

The relationship between active layer thickness and device transmittance in **Figure 4b** demonstrates that the thinnest active layer film yields a high transmittance. On the other hand, the device efficiency increases with increased thickness, as shown in **Figure 4c**, up to 100 nm. Layers thicker than 100 nm result in decreased efficiency with lower fill factor values, possibly due to increased series resistance or optical effects. On average, the 53 nm thin film produced the highest AVT at a constant Ag electrode thickness, and the thickest film, at 143 nm, resulted in the lowest AVT, as demonstrated in **Figure 4d**.⁵⁹ As such, the AVT values are significantly affected by film thickness. However, the active layer thickness can vary depending on the absorption coefficient of the active materials. As active materials significantly influence the PCE, their absorption coefficient is also critical for determining the AVT. The PCE and AVT are important for achieving high LUE. Therefore, it is crucial to understand the relationships among active materials, PCE, AVT, and LUE, a few of which are highlighted in **Table 2**. However, a comprehensive summary can be found in the literature^{65,66}.

Table 2: Some materials composition for ST-OPVs with their PCE, AVT/APT, and LUE values.

Active layer	PCE (%)	AVT/APT (%)	LUE (%)	Ref.
PTB7-Th:IUIC	10.2	31.0	3.16	67
PTB7-Th:IHIC	9.8	36.0	3.52	68
PTB7-Th:FOIC	10.3	37.4	3.85	69
PTB7-Th:IEICO-4F	10.0	34.2	3.42	70
PTB7-Th:A078	10.8	45.7	4.94	71
PTB7-Th:H3	8.4	50.1	4.06	27
PM6:Y6	12.9	25.6	3.30	72
PM6:Y6	9.4	42.8	4.02	73
PM6:Y6	13.7	22.2	3.04	74
D18:Y6	12.3	17.0	2.09	75
D18:N3	12.6	22.8	2.87	76
PM6-BTP-eC9:L8-BO	11.4	46.8	5.34	77
PBDB-TF:L8-BO:BTP-eC9	13.0	38.7	5.03	78
PTB7-Th:PBDB-T:PC ₇₁ BM:ITIC-Th	7.9	63.0	4.98	26

The transmittance of an OPV is also dependent on other internal device layers, such as the electrodes. **Figure 5** shows the relationship between device performance and AVT for PBDB-T:ITIC devices from the same study with variable Ag electrode thicknesses.⁵⁹ Multicomponent electrodes, such as MoO₃/Ag/MoO₃, helped in effective light management for improved performance. As the electrode thickness increased, the current increased, as shown in **Figure 5a**. A similar trend was also observed in the external quantum efficiency measurement shown in **Figure 5b**. The thicker cathode layers decreased transmittance and the AVT, as shown in **Figures 5c** and **5d**.⁵⁹ Details on multicomponent electrodes, including their limitations, are discussed in section 4.

The drive to study other non-fullerene acceptors designed to capture near-infrared spectra then marked the birth of the Y-series acceptor.⁷⁹ To increase the degree of conjugation and enhance



molecular charge transfer in ITIC, Yang et al. inserted the sp^2 -N group, further delocalizing electrons and a redshift in the molecular absorbance seen in **Figure 6a**. This discovery enabled the creation of Y1, Y2, and Y6 acceptor molecules. Y6 in OPV devices led to an increased efficiency of 15.7%.⁸⁰ In a PM6:Y6 active layer blend, the AVT is 26% and has been shown to increase to 60% at a thickness of 100 nm upon adding a ternary molecule, BFSN, shown in **Figure 6b**.⁸¹ This additive led to a reduction in the efficiency of the devices from 12.8% to 11.8%.⁸¹ The broad relationship between efficiency and AVT is shown in **Figure 6(c)** amongst many design strategies.

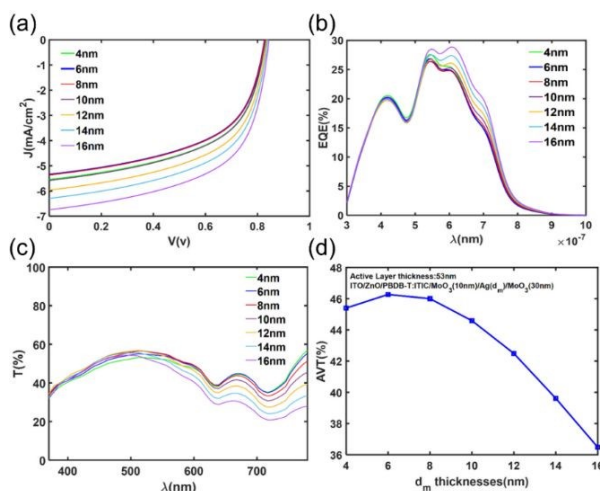


Figure 5. (a) Performance parameters for the ITO/ZnO/PBDB-T:ITIC/MoO₃/Ag/MoO₃ structure with varying cathode thickness of $d = 4, 6, 8, 10, 12, 14, 16$ nm. (b) Metal thickness relative to external quantum efficiency. (c) transmission relative to metal thickness. (d) AVT over the range of tested metal thickness. Reproduced with permission.⁵⁹ Copyright 2022, Scientific Reports.

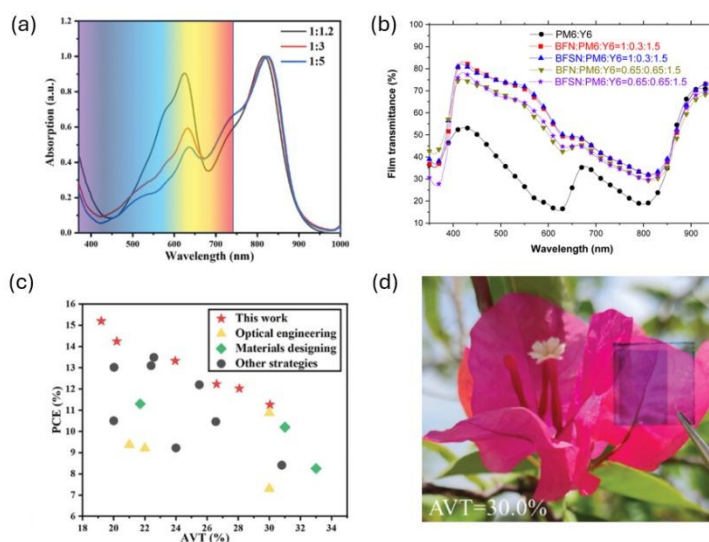


Figure 6. (a) Normalized absorption spectra of PM6, Y6-BO, and 2PACz demonstrating infrared device absorption. Reproduced with permission.⁸⁰ Copyright 2022, Advanced Energy Materials. (b) Percent film transmittance of ITO/PEDOT:PSS/BFSN, PM6, Y6. Reproduced with permission.⁸¹ Copyright 2022, Scientific Reports. (c) The relationship between device architecture and AVT considers optical engineering, materials design, other strategies,



and the work presented by Jing et al.⁸⁰ **(d)** Thin film held up next to a flower, demonstrating an AVT of 30%. Reproduced with permission.⁸⁰ Copyright 2022, Advanced Energy Materials.

The trade-off in the relationship between AVT and efficiency is calculated in the LUE so that new semitransparent technologies can be compared. One study found that a ternary system with a polymer donor, cyclopentadithiophene, and acceptor has the highest reported near infrared LUE value of 4%.⁸² In order to achieve an optimized agrivoltaics system, a high AVT and efficiency in ST-OPV systems must be achieved and further studied for crop use. **Figure 6d** demonstrates what an AVT of 30% would look like over a flower specimen. Further plant and device research should report the average photosynthetic transmittance to optimize future agrivoltaic systems.

3.2 Semitransparent PPVs

PPVs are a rapidly advancing technology with improvements in efficiency from 3.8%⁸³ to over 26%^{34,35,84} in recent years. This progress is attributed to their intrinsic material properties, such as a high optical absorption coefficient, enhanced carrier mobility, and extensive carrier diffusion length.^{85–87} Advanced techniques, including interface engineering, carrier management, and additive engineering, have further influenced the rapid progress.^{88,89} The unprecedented growth of the PPVs is also associated with their ambient and solution processability at low temperatures below 200°C.^{90–92} This contributes to the economic viability of this groundbreaking PV technology. Furthermore, their solution processability makes PPVs compatible with flexible substrates like polyethylene terephthalate. The crystal structure of perovskites with an ABX₃ formula is illustrated in **Figure 7a**, where X is an anion and A and B are cations of differing sizes, with A being larger in radius.⁹³

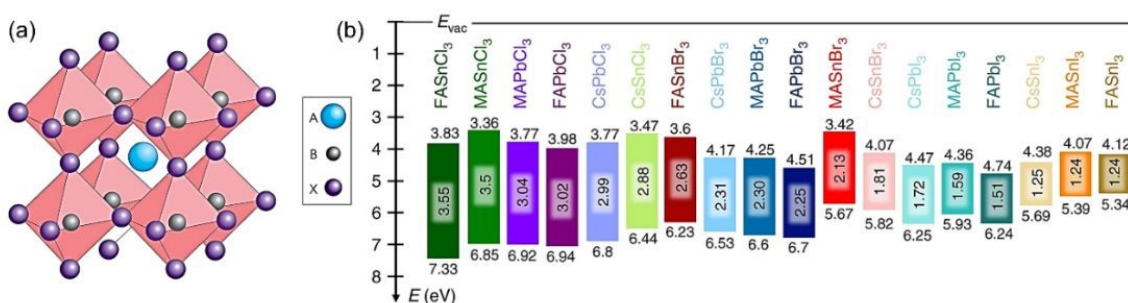


Figure 7. (a) Cubic perovskite crystal structure. Reproduced with permission.⁹³ Copyright 2014, Macmillan Publishers Limited. (b) Energy level diagram of the 18 metal halide perovskites. Reproduced with permission.⁹⁴ Copyright, Nature Communications.

Through the compositional engineering in the structure, the bandgap of perovskite materials can be tuned from 1.2 to 3.5 eV, as shown in **Figure 7b**.⁹⁴ Through this bandgap engineering, the absorption range of perovskite materials can be adjusted for the application of agrivoltaics for specific species of plants. Like ST-OPVs, PPVs can also be utilized as ST-PPVs by controlling their composition or thickness.⁵⁰ A study by Shi et al. investigated ST-PPVs using a wide-



bandgap perovskite composed of $\text{Cs}_{0.2}\text{FA}_{0.8}\text{Pb}(\text{I}_{0.6}\text{Br}_{0.4})_3$.⁴⁹ The concentration of perovskite was varied from 0.2M to 1.0M to obtain different levels of transmittance influenced by varying film thickness. Perovskite films exhibited optimal transparency at lower concentrations, as shown in **Figure 8a**. The thicknesses of the perovskite layers corresponding to concentrations of 0.2, 0.4, 0.5, 0.6, 0.8, and 1.0M are 110, 197, 252, 291, 362 and 440 nm, respectively. The device efficiency increased from 10.2% to 14.8% as thickness increased from 252 nm to 440 nm (efficiencies for devices with 110 nm and 197 nm thickness layers were not obtained). The transmittance spectra of ST-PPVs with a device architecture of ITO/NiOx/perovskite/ C_{60} /BCP/ITO are presented in **Figure 8b**. The AVT for these perovskite films was calculated over the wavelength range between 400 nm and 800 nm. The introduction of surface modification on NiOx, a hole transport layer, with 2PACz enhanced the alignment of work function within the device. By optimizing the thickness of ITO as a top transparent electrode, a high efficiency of 14.4% was achieved for ST-PPVs, with an AVT of 38%, as depicted in **Figure 8c**. From this data, the LUE value is calculated to be $\sim 5.5\%$, notably higher than other referenced studies.

Yu et al. also explored ST-PPVs, focusing on key factors affecting the device performance and stability through the compositional modification of $\text{APbI}_x\text{Br}_{3-x}$ (A = CsFAMA, CsFA, and MA) perovskites.⁹⁵ The influence of modification at A- and X-site within APbX_3 perovskites on performance and stability was critically assessed. **Figure 8d** demonstrates that the perovskite films showed varying compositions at the A-site and X-site. The abbreviation from A-1 to A-4 indicated an increase in the ratio of Br to I from 0.51 to 1.95. Interestingly, an increase in the Br ratio at the X-site resulted in higher transmittance and a shift in the bandgap from 1.63 to 1.92 eV. ST-PPVs with CsFA-2 perovskite, with a band gap of approximately 1.74eV, were fabricated with a perovskite layer thickness ranging from 100 nm to 400 nm. The transmittance significantly increased below 700 nm with decreasing thickness, as shown in **Figure 8e**. These findings underscore the potential of ST-PPVs in agrivoltaic applications, where high transmittance and device performance are crucial. The trends in efficiency and AVT discussed here, along with other references represented in **Figure 8f**, highlight that the LUE value exceeds 4%, demonstrating the promising capabilities of ST-PPVs in integrating agricultural and photovoltaic applications effectively.



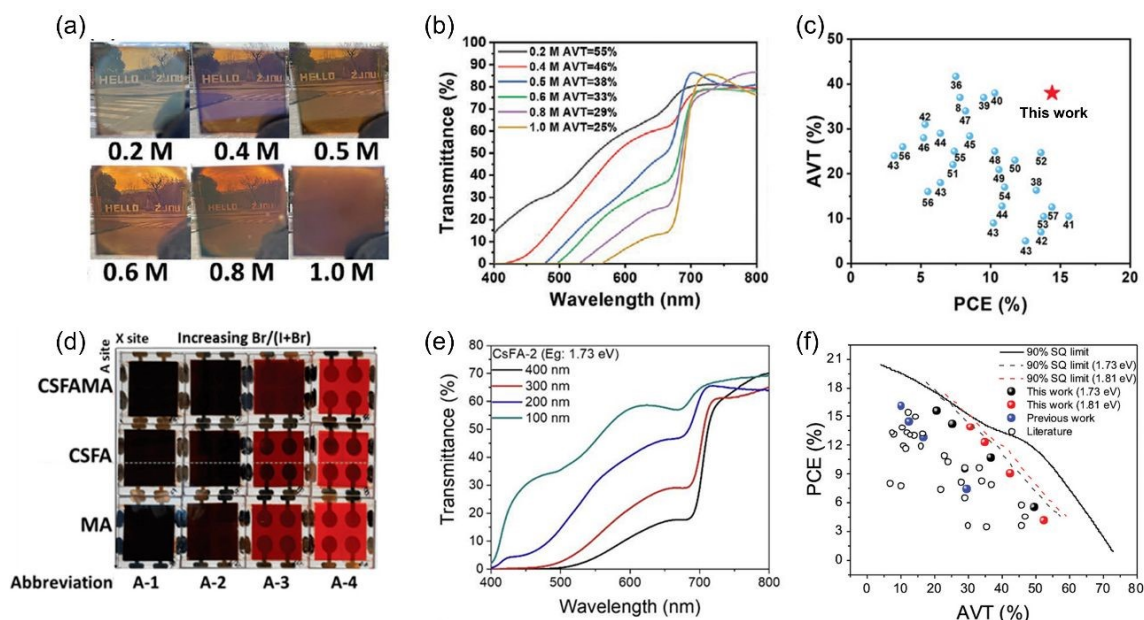


Figure 8. (a) Perovskite films with different molar concentrations. (b) Transmittance spectra of ST-PSCs with different concentrations. (c) Comparison of AVTs and efficiencies with other works. Reproduced with permission.⁴⁹ Copyright 2022, Wiley-VCH GmbH. (d) Perovskite devices with different color tunability through control of the cation such as MA, FA, and Cs and halides such as iodide and bromide compositions. (e) Transmittance spectra of ST-PPVs with different film thicknesses of CsFA-2 film. (f) Efficiencies and AVTs of their previous work and with literature. Reproduced with permission.⁹⁵ Copyright 2022, Wiley-VCH GmbH.

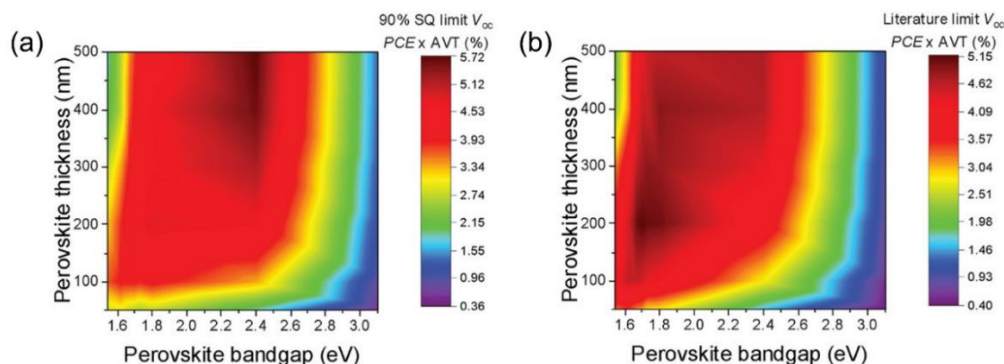


Figure 9. The maximum theoretical efficiency of ST-PPVs is determined by LUE ($PCE \times AVT$), using efficiency values calculated from (a) V_{oc} at 90% of the Shockley-Queisser limit and (b) the highest V_{oc} related to the band gap reported in the literature. Reproduced with permission.⁹⁵ Copyright 2022, Wiley-VCH GmbH.

In **Figure 9a**, Yu et al. introduced the maximum theoretical LUE value predicted for the perovskite films.⁹⁵ The inputs for these LUE calculations for ST-PPVs were estimated using a transfer matrix method and by assuming a voltage at 90% of the value predicted by the Shockley-Queisser limit. Simulation results indicate that the highest LUE value is 5.7%, with an ideal band gap of approximately 2.4 eV and film thicknesses of about 250 nm and above. Meanwhile, the LUE map based on the reported literature showed the highest LUE at around 5.2% with 1.7 eV of bandgap and 200 nm of film thickness, as illustrated in **Figure 9b**. However, along with the importance of LUE, the specific absorption wavelength is particularly significant for agrivoltaic applications. This



absorption region will be discussed in the following section. Other forms of controlling PPV transparency can be achieved through translucent devices without compromising the efficiency and aesthetics required for platform integration, such as buildings.⁹⁶ Various translucent devices, including cells and modules, manufactured with laser-induced micro-patterning demonstrate how new module designs can meet the optical LUE objectives for building integration.⁹⁶ This could be potentially further explored for agrivoltaics.

3.3 Utilizing ST-OPVs and ST-PPVs in Agrivoltaic Systems

To incorporate ST-OPVs and ST-PPVs into agrivoltaic systems, the known photosynthetic active radiation for the targeted crop species is required. The absorption spectra of major plant photosynthetic pigments and active materials in ST-PVs are depicted in **Figure 10**. Each graph highlights the green wavelength range (500-600 nm) for simple visual comparison. On average, single leaves have high absorptivity in the photosynthetic active radiation range (85%) and low absorptivity in the near-infrared (15%). According to **Figure 10a**, key pigments such as Chlorophyll A, which is predominant in many plants, absorb primarily in blue and red regions of the spectrum, whereas Chlorophyll B also absorbs these wavelengths but within a narrower range. Although minimal, plants rich in carotenoids will also absorb blue-green radiation.⁹⁷

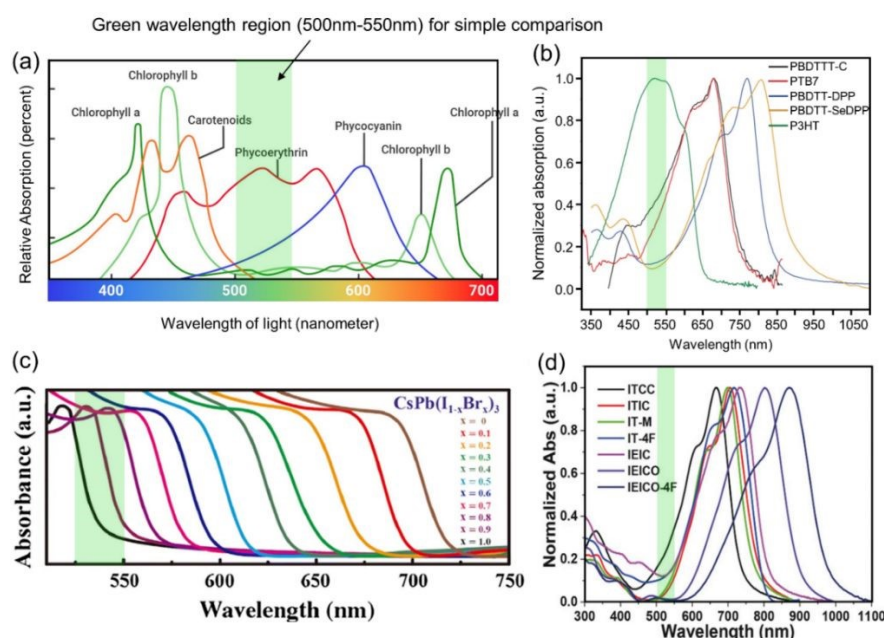


Figure 10. Absorption spectra of (a) plant photosynthetic pigments. Reproduced with permission.¹⁰² Copyright 2020, CircuitBread, (b) donor materials for ST-OPVs. Reproduced with permission.¹⁰³ Copyright 2015, Macmillan Publishers Limited, (c) all inorganic CsPb(I_{1-x}Br_x)₃ perovskite for ST-PPVs. Reproduced with permission.¹⁰¹ Copyright 2020, Springer, and (d) acceptor materials for ST-OPVs. Reproduced with permission.¹⁰⁴ Copyright 2018, WILEY-VCH Verlag GmbH & Co. KGaA, Weinheim.

The light and energy ratios plants are exposed to matter for their ultimate growth. Blue light, for example, is important for early development phases in plants, promoting processes like stomatal



opening and stem growth, while red light facilitates flowering and bud formation. Green light exposure has demonstrated a potential increase in leaf growth and biomass production despite plants having low absorption of this wavelength.⁹⁸ In nature, green light absorption may also be used in plants as a signaling mechanism for leaf inclination. In addition, early stem elongation, leaf growth, stomatal conductance, and plant biomass are each stimulated by a minimal degree of green light exposure.⁹⁹ Considering these requirements, photoactive materials in ST-PVs that absorb the NIR and allow blue and red-light transmission are typically preferred for plant growth. As shown in **Figure 10b** and **d**, organic donor and acceptor materials for ST-OPVs mostly absorb light at a wavelength longer than green, making them suitable for transmitting blue light to the crops. In terms of the red spectrum, donor materials like P3HT, PDBTT-DPP, and PBDTT-SeDPP, and acceptor materials such as IEIC, IEICO, and IEICO-4F, are particularly suitable for agrivoltaics systems as the active material's absorption spectra do not interfere with that of major light-harvesting pigments in plants. Meanwhile, materials such as PTB7, PBDTTT-C, ITCC, ITIC, IT-M, and IT-4F, which absorb in the red regions, could also be effectively utilized. A recent study reported an upscaled PM6:PYTF blend OPV for agrivoltaic application, demonstrating adequate light transmission properties (with AVT between 36 and 45%) and an overview of the observed device degradation from various greenhouse stressors.¹⁰⁰

For ST-PPVs, the absorption edge can shift with changes in the perovskite composition.¹⁰¹ For instance, **Figure 10c** shows the absorption spectra of $\text{CsPb}(\text{I}_{1-x}\text{Br}_x)_3$ perovskite materials at different bromide to iodine ratios. With values of $x = 0.9$ or 1.0 , the absorption edge appears near the green region, shifting towards red as the bromide ratio decreases. Perovskite materials have a broader absorption range than organic materials, exhibiting sharp peaks in specific regions. This versatility benefits their use in PV applications, although it may restrict their suitability in agrivoltaics for diverse plant species.

3.4 Agrivoltaic Greenhouse Applications: Crop Shading

As previously stated, the success of ST-OPVs and ST-PPVs depends heavily on the light and thermal requirements of the crop species. Shading has already been explored for various reasons, such as reducing the crop's evapotranspiration rates to conserve water and lowering the air temperature in the greenhouse to mitigate plant stress.^{105–107} This section specifically discusses case studies of integrated ST-PV systems and the partial shading effects in greenhouse structures regarding crop yield across the globe. Other semitransparent systems, such as dye-sensitized solar cells, amorphous silicon, CdTe, etc., have been applied to agrivoltaic systems as well; thus, this section highlights the diversity of ongoing work.^{108,109}

One shading study conducted by Cossu et al., based on commercial installations in Sardinia, Italy, discussed the shadowing dynamics in greenhouses using various ratios of opaque silicon PV cover ratios.¹¹⁰ This study demonstrated that high light-demanding crops such as tomato, sweet pepper, and cucumber reached optimal crop yield with a 25% overhead shading cover ratio. Medium light-demanding species in the same research study found that basil, spinach, strawberry, and lettuce yield also remained consistent below this 25% crop shading threshold, as shown in **Figure 11**. Low-light floricultural plants, dracaena, kalanchoe, and poinsettia, also demonstrated high



yields across all photovoltaic coverage levels. With a 32-100% crop cover ratio, raspberry, wild strawberry, and blueberry each demonstrated higher antioxidant levels, illustrating one aspect of the nutritional value that shading can contribute to precision growth.¹¹⁰

In addition, a separate study conducted in Brazil reported that the total dry mass of tomato fruit in a control versus a treatment with a 52% shading screen was 550 and 420 g.m⁻², respectively.¹¹¹ However, a case study in Kunming, China, tested monocrystalline silicon ST-PV systems covering over 20% of greenhouse rooftop structures, showing no significant differences in tomato growth.¹⁴ Thus, up to 20 to 25% of the incoming solar radiation could be diverted to electricity without affecting the yield of some horticultural crops.

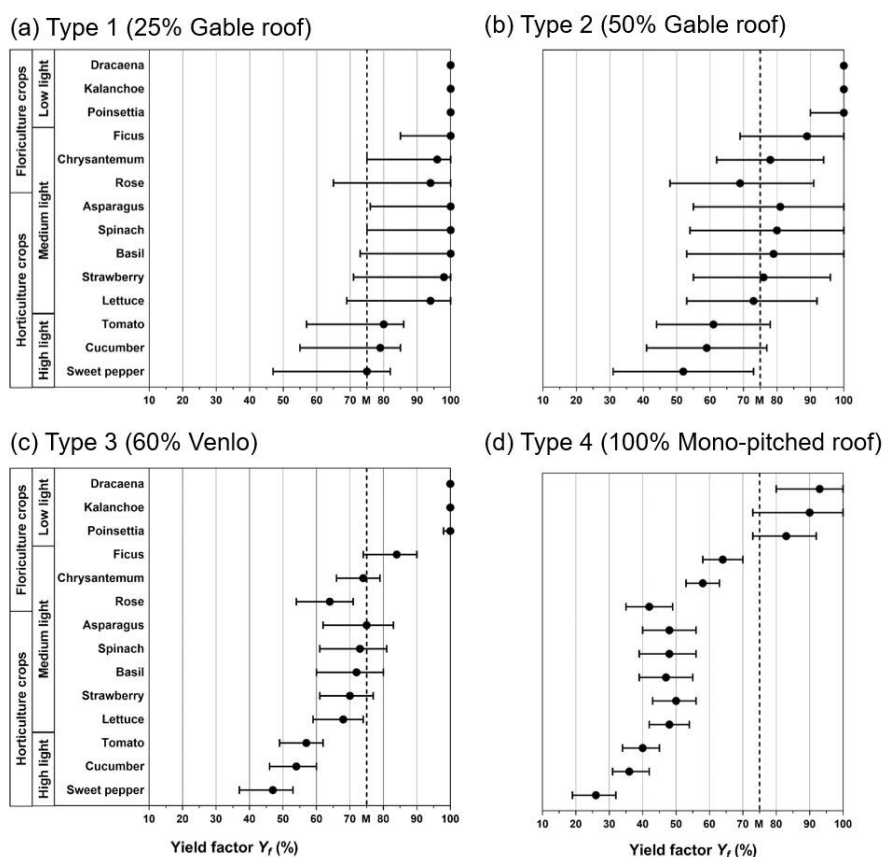


Figure 11: Comparison of the four silicon PV greenhouse shading types based on total cover ratio, 25%, 50%, 60%, and 100% (a,b,c,d respectively) in Sardinia, Italy versus calculated yield according to the plants required daily light integral. The M value on each graph represents the minimum acceptable yield factor on a yearly basis. Reproduced with permission.¹¹⁰ Copyright 2020, ScienceDirect.



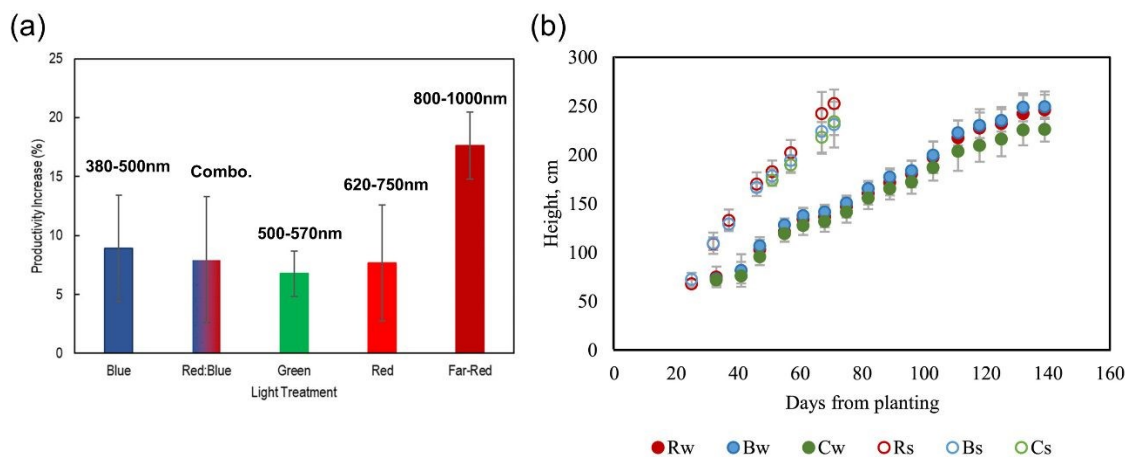


Figure 12: (a) Productivity increase (mean of leaf area, leaf number, biomass, height) due to changes in LED light quality for horticultural crops (e.g., spinach, rocket, lettuce) from a control “white” light source. Wavelengths were provided as an estimated approximation. Reproduced with permission.¹¹² Copyright 2023, HortScience. (b) Plant height as a function of days from planting. R, Greenhouse with Red OPV modules; B, Greenhouse with blue OPV modules; C, Control Greenhouse; Subscripts w and s refer to summer and winter seasons. Reproduced with permission.¹¹³ Copyright 2023, ScienceDirect.

The integration of ST-OPVs and ST-PPVs as radiation-harvesting layers over greenhouse structures represents a novel approach in agrivoltaic technology. Due to their unique light transmission capabilities, reporting an AVT is essential when performing an agrivoltaic research study. **Figure 12a** demonstrates how certain colors may affect crop productivity,¹¹² while **Figure 12b** compares tomato crop height under red vs blue ST-OPV modules.¹¹³ In a pioneering study on agrivoltaic OPV integration, devices with an approximate 20% measured transmissivity covered 37% of the greenhouse roof area while researchers examined microclimate, yield, and physiological parameters.¹¹⁴ Results showed a higher leaf area index, average fruit mass, and cumulative yield in the OPV system compared to the 25% black-shaded control system, with no significant differences in the following year.¹¹⁴ The reported AVT spectrum for this module peaked at 475nm and 720nm.¹¹⁵

Another study using dye-sensitized solar shading (without precise transmissivity data) presented lower early yields, stomatal conductance, and photosynthetic rates for tomato plants but found improved fruit quality, such as increased sugar content.¹⁰⁹ In Kitzingen, Germany, an agrivoltaic research team reported red and blue OPV greenhouse transmittance values of 32.2 and 28.8%, covering 27.3 and 26.8% of the ground area, respectively. Their findings show faster tomato growth under OPV shading, although the accumulated yield was higher in the control system (see **Figure 12b**).¹¹³ Furthermore, Gnayem et al. compared silicon glass, plastic, and organic solar cells in greenhouses producing cucumbers in Kfar, Israel, and revealed the potential of OPV modules to balance energy production and crop growth.¹¹⁶

Precision farming techniques can also use models to predict the overall crop yield or mass and the energy generation under various OPV cover ratios and angles for multiple agrivoltaic systems. In Tucson, AZ, USA, an agrivoltaic model was able to accurately predict lettuce crop shoot weight and estimate the yearly electric energy generated at 8.9 kWh.m⁻².year⁻¹ with 25% OPV coverage and a 3.3% efficiency.¹¹⁷ Scientists found that the developed model predicted that 49% OPV



coverage was sufficient to meet the total energy demand of the greenhouse.¹¹⁷ This kind of predictive modeling is useful for farmers to estimate the energy yield and operational costs of implementing ST-OPV technology over various climate environments. Other methods to assess OPV arrays in greenhouses have been investigated.¹¹⁸ Future research analyzing the relationship between the AVT of the ST-PV devices and crop yield data needs to be reported to demonstrate the benefits of selective and reliable ST-PV integration into agrivoltaic systems.

4. Limitations of Semitransparent PVs

Stability: Although OPVs and PPVs have seen significant efficiency improvements, long-term stability remains a challenge as they are susceptible to oxidation, high temperature, and their relatively delicate chemical bonds compared to conventional inorganic PVs.^{119,120} Therefore, understanding their fundamental degradation mechanism is essential. Different degradation factors include the metastable morphology of the photoactive layer, diffusion of electrodes and buffer layers, oxygen and moisture, illumination, heating, and mechanical stress.¹²¹ For OPVs, the organic materials themselves can degrade through photo-oxidation when exposed to oxygen and sunlight. The bulk heterojunction morphology can also undergo severe phase separation, significantly increasing non-geminate recombination and decreasing efficiency.¹²² Furthermore, the interface stability between the active layer, transport layers, and electrodes is also critical, as any of these interfacial degradation mechanisms can reduce the charge carrier mobility and, therefore, the overall efficiency of the device.¹²³ In the case of PPVs, stability issues are often attributed to the sensitivity of perovskite materials to moisture, heat, and UV radiation.¹²⁴ Perovskite can degrade into its constituent components when in contact with moisture, leading to a loss in its absorption properties. Thermal instability can also cause structure changes within the perovskite layer, affecting the electronic properties and leading to efficiency losses.¹²⁴ UV stability is another concern, as prolonged exposure can alter the composition of perovskite materials. To solve these stability issues, considerable research is needed on developing stable electrode materials, synthesizing more robust organic and perovskite compounds, and/or enhancing encapsulation techniques.

Transparency and stability of top electrodes: Another limitation of ST-PVs involves the low transmittance of the top electrodes made from evaporated materials such as aluminum, silver, or gold. To increase their transmittance, the thickness of these electrodes can be reduced. However, this reduction in thickness can significantly increase their electrical resistivity, negatively affecting efficiency. This situation requires considering a trade-off between the electrode thickness and efficiency, similar to the compromise made between the thickness of the active layer and efficiency. As illustrated in **Figure 13a**, there is a noticeable drop in transmittance when the electrode thickness exceeds 20nm.¹²⁵ Conversely, the resistivity of a silver electrode begins to increase dramatically when the thickness falls below 10nm, as shown in **Figure 13b**.



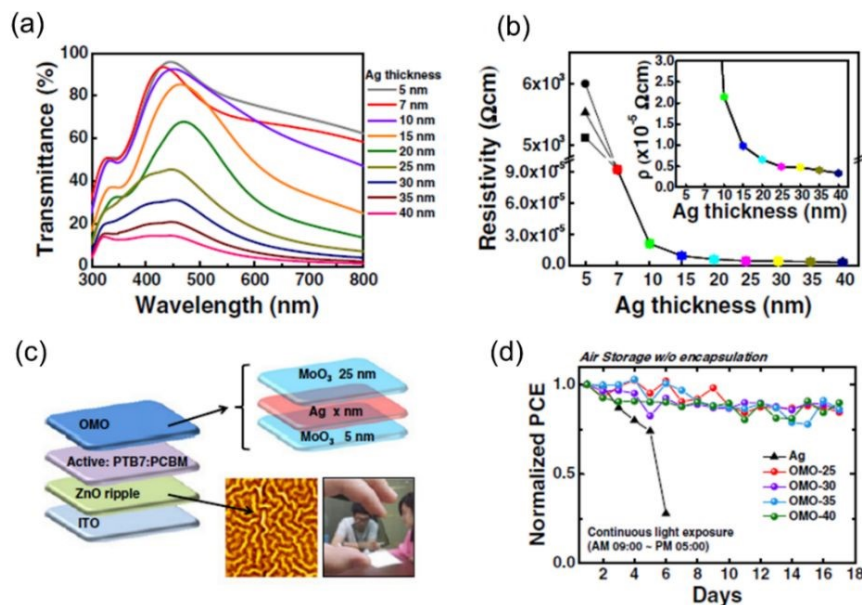


Figure 13. (a) Transmittance and (b) resistivity of silver electrodes with various thicknesses. (c) Device configuration, and (d) device stability with oxide-metal-oxide structure in air without encapsulation. Reproduced with permission.¹²⁵ Copyright, 2017 John Wiley & Sons, Ltd.

In practice, a thickness of 25nm is selected for optimal device performance, achieving an efficiency of 8.4%. Additionally, thinner silver layers are more susceptible to degradation. An oxide-metal-oxide structure is introduced to address this issue, as demonstrated in **Figure 13c**.¹²⁵ This structural modification has been proven to significantly enhance device stability when exposed to air, unlike devices with only silver, which degrades much faster. This rapid degradation of silver-only electrodes is depicted in **Figure 13d**. Although such evolving techniques improve the transparency and stability of the top electrodes, these thermally evaporated top electrodes are still one of the biggest hurdles to their commercialization. Therefore, it is essential to develop an alternative method for the commercialization of fully solution-processable top electrodes.^{126–128}

Solvent toxicity and lead leaching: Device toxicity is also a significant concern, especially for agricultural applications. Solution processing of OPVs and PPVs often uses toxic solvents, including halogenated and aromatic hydrocarbon solvents like chlorobenzene, chloroform, and dimethylformamide. To address this issue, research is intensively focused on environmentally benign solvents for processing OPVs/PPVs, such as 2-methyl-tetrahydrofuran and N-methyl-pyrrolidone.¹²⁹ One approach to developing eco-friendly solvent-processed OPVs/PPVs is to test alternative solvents for well-established materials. Another widely applied method is modifying the structure of well-established molecules while maintaining key properties like charge transport, molecular packing, absorption coefficient, and carrier mobilities.¹³⁰

Regarding toxicity, potential lead (Pb) leaching from lead-based PPVs is also recognized as a major environmental concern for large-scale commercialization. Pb plays a crucial role in PPVs as an ideal divalent cation with suitable ionic radii and an ideal electronic configuration, such as Pb 6s



lone-pair states and Pb 6p orbitals.¹³¹ However, Pb is considered a health hazard and a harmful element for both natural and built environments.¹³² Yan et al. conducted quantitative research on lead leaching in five benchmark PPVs: MAPbI₃, FA_{0.95}MA_{0.05}Pb(I_{0.95}Br_{0.05})₃, Cs_{0.05}(FA_{0.85}MA_{0.15})_{0.95}Pb(I_{0.85}Br_{0.15})₃, CsPbI₃, and CsPbI₂Br.¹³³ Rapid Pb leaching was observed, with more than 60% of the total Pb leaching from the PPVs within the first 120 seconds of aqueous exposure. The Pb leaching process was found to vary depending on the moisture stability, film quality, and total Pb amount in the film. To mitigate this issue, researchers are increasingly focusing on developing Pb-free PPVs and PPVs with reduced amounts of Pb, such as ASnX₃ tin perovskites, A₂B(I)B(III)X₆ double perovskites, and Sn/Pb mixed perovskites.^{134,135} However, Sn-based PPVs, with an efficiency above 14%,^{136,137} are significantly behind their Pb-based counterparts and are also unstable. Also, Sn-based PPVs could also be problematic in terms of health and safety. Therefore, it is important to develop new methods to improve both the performance and environmental stability of Pb-free PPV devices to meet IEC qualification standards.^{138,139} Recently, new approaches such as lead chelation and adsorption have been explored to maintain device performance with lead while preventing lead leaching upon damage.^{140,141} For instance, Fei et al. investigated a lead chelating hole transport layer that can strongly interact with lead ions, resulting in a high PCE of 21.8% for a minimodule with an area of 26.9 cm².¹⁴² In addition, Zhang et al. introduced lead immobilization methods that transform water-soluble lead ions into insoluble, non-bioavailable, and non-transportable forms over a wide range of pH and temperature conditions.¹⁴³ These methods include grain encapsulation, lead complexation, structural integration, and lead adsorption. Combining multiple strategies is suggested to achieve higher lead sequestration efficiencies.

The scientific community is divided about the use of Pb in PPV technologies. There are two schools of thought on the matter. Some judge that the amount of Pb in the conceived potential technology is acceptable. It would be much less than current Pb-based technologies such as lead-acid batteries, solder, cathode-ray tube glass, and waste-printed circuit boards.^{144,145} Others consider that PPVs present a danger to people in manufacturing, the environment, and end users. Though this may not be a direct comparison in terms of volumetric content, it is believed that the average amount of lead, for instance, in current lead-acid batteries is about 10 kilograms¹⁴⁶, which far exceeds the stipulated lead content in PPV panels. For comparison, the amount of lead is estimated to be about 1 gram per 1 m² size panel.¹⁴⁷ Thus, in this regard, they believe the Pb content is not significant, especially when PPVs are packaged, sealed, and encapsulated to avoid Pb leaching. For agrivoltaics/greenhouse applications, we side with the second school of thought as the idea of Pb leaching in agricultural environments, which, to any degree, would pose a risk to the health of our communities.

5. Perspective

Although many studies suggest the application of ST-PVs for agrivoltaics, there is still a lack of direct research focused on ST-OPV and ST-PPV agrivoltaic greenhouse integration. The implementation of ST-PVs in agrivoltaics or greenhouse systems is still in its early stages, which provides an opportunity to foster increased agrivoltaic research.



However, semi-transparent luminescent solar concentrator designs have been tested and are ready for greenhouse applications. They have low power conversion efficiencies of 7%.^{17,148} Various designs are adapting to new research suggesting that quantum dots, organic dyes, and reflective surface geometries can increase light extraction for improved system performance.¹⁴⁸ Further work into the discussed limitations will soon initiate these advances to become a part of our everyday lives. In the meantime, expanding our library of optimal photosynthetic plant growth conditions under various filters and reporting AVT values can help us narrow down the most desirable systems. Due to the potential toxicity of perovskite materials, as discussed, and issues like microplastic waste, ensuring the health and safety of the agrivoltaic food we consume needs to be a priority. Despite these existing challenges related to OPVs and PPVs, recent advancements in the field have shown promising developments. A noteworthy example is Heliatek's recent success in achieving IEC 61215 ageing certification for the first time in OPV technology for their flexible product, HeliaSol.¹⁴⁹ This industry standard defines the design and qualification of silicon PV modules for long-term operation in open-air, terrestrial applications. This certification is significant as it confirms the durability of flexible OPV, marking it the first commercially available in the HeliaSol series of OPV products to meet such rigorous standards. The certification by TÜV Rheinland underscores Heliatek's technological advancement and boosts confidence in OPVs for more demanding installations globally. For PPVs, they were recently shown to pass the (i) IEC 61215:2016 thermal cycling test for FAPbI_3 -based cells¹⁵⁰, (ii) IEC 61215:2016 damp heat and humidity freeze tests for $\text{Cs}_{0.05}\text{FA}_{0.8}\text{MA}_{0.15}\text{Pb}(\text{I}_{0.85}\text{Br}_{0.15})_3$ and $\text{FA}_{0.85}\text{MA}_{0.15}\text{Pb}(\text{I}_{0.85}\text{Br}_{0.15})_3$ -based cells¹⁵¹, (iii) IEC 61215:2016 damp heat test, thermal cycling test, and ultraviolet preconditioning test, for $(5\text{-AVA})_x\text{MA}_{1-x}\text{PbI}_3$ perovskite-based cells, exhibiting over a 9 000 hours of operational stability¹⁵², in a lab. Environment; and (iv) IEC 61215/61730 at industry level, by Microquanta¹⁵³. With crop yields increasingly affected by climate change, these certifications for OPV and PPV design represent a milestone in potentially meeting the agrivoltaic goals we see in the future.

6. Conclusion

There remains a demand for integrating renewable energy devices into agricultural land use. The unique properties of emerging thin-film semitransparent organic and perovskite photovoltaics, such as transparency and tunability, make them particularly promising for agrivoltaics. For instance, these solar modules can be integrated into greenhouse rooftops, allowing selective light transmission to ensure appropriate wavelengths for plant growth while converting excess light into electricity. This review highlights the potential of integrating ST-PV systems into greenhouse applications with key metrics such as AVT, LUE, and efficiency. Current research indicates that ST-OPVs and -PPVs offer 10-50% of AVT values and efficiencies of around 5-17%. Considering the trade-off between efficiency and AVT, the LUE metric is crucial to demonstrate the potential of these technologies. In summary, LUE values reach 5% for ST-OPVs and 5.5% for ST-PPVs. In comparison, the most efficient luminescent solar concentrator device had a much lower LUE value of only 2.6%.¹⁷ Although seemingly inefficient, luminescent solar concentrator devices can offer much longer stability properties than current OPV or PPV systems, potentially favorable for current dual-land use integration. Although a high LUE value is generally desirable



for agrivoltaic applications, it is not always the sole factor, as spectral engineering plays a crucial role in optimizing light absorption for agricultural productivity. In this review, we compared the absorption characteristics of ST-PVs with different photoactive materials and compositions to the absorption spectra of various plant light-absorbing pigments, such as chlorophyll A, chlorophyll B, and carotenoids. This comparison provides insights into spectral engineering required for agrivoltaic applications tailored to different plant species. In addition, we discussed the current limitations of these techniques, such as stability and toxicity for agricultural applications. Further research in photoactive materials, encapsulation techniques, and compositional engineering is required to integrate ST-PVs into agrivoltaic systems. Investigating crop shading and device performance will soon play a pivotal role in transforming agricultural practices, supporting both clean energy production and sustainable agriculture. The InSPIRE team, supported by the U.S. Department of Energy, has developed an interactive agrivoltaic map and calculator to explore current agrivoltaic projects in the United States and assess the nationwide feasibility.¹⁵⁴ In the future, we look forward to ongoing advancements in ST-OPV and ST-PPV agrivoltaic systems around the world, aiming to benefit a growing society and preserve our natural environment.

Conflicts of interest

There are no conflicts to declare.

Acknowledgments

N.R. and E.D.G. acknowledge funding support from the U.S. Department of Defense, Army Research Laboratory, and Army Research Office under grant number W911NF-23-2-0. N.Y.D. acknowledges support from the Materials Research Institute (MRI) and the Institute of Energy and the Environment (IEE) of The Pennsylvania State University, University Park. A.K. was supported by the USDA National Institute of Food and Agriculture and Hatch Appropriations under Project #PEN05001 and Accession #7007612.

Reference

- 1 U.S. energy consumption increases between 0% and 15% by 2050 - U.S. Energy Information Administration (EIA), <https://www.eia.gov/todayinenergy/detail.php?id=56040>, (accessed June 28, 2024).
- 2 M. C. Hunter, R. G. Smith, M. E. Schipanski, L. W. Atwood and D. A. Mortensen, *BioScience*, 2017, **67**, 386–391.
- 3 R. M. Beyer and A. Manica, *Nat Commun*, 2020, **11**, 5633.
- 4 Ocean Acidification, Today and in the Future | NOAA Climate.gov, <https://www.climate.gov/news-features/featured-images/ocean-acidification-today-and-future>, (accessed June 28, 2024).



- 5 Almond R.E.A., Grooten M, Juffe Bignoli, D. & Petersen, T. (Eds), *Living Planet Report 2022 – Building a nature-positive society.*, WWF, Gland, Switzerland.
- 6 K. A. Naylor, *UN-Water, Blueprint for acceleration : sustainable development goal 6 synthesis report on water and sanitation, 2023*, United Nations, New York, 2023.
- 7 *Inventory of U.S. Greenhouse Gas Emissions and Sinks 1990-2022*, U.S. Environmental Protection Agency, EPA 430R-24004, 2024.
- 8 J. Macknick, H. Hartmann, G. Barron-Gafford, B. Beatty, R. Burton, C. Seok Choi and Matthew Davis, Rob Davis, Jorge Figueroa, Amy Garrett, Lexie Hain, Stephen Herbert, Jake Janski, Austin Kinzer, Alan Knapp, Michael Lehan, John Losey, Jake Marley, James MacDonald, James McCall, Lucas Nebert, Sujith Ravi, Jason Schmidt, Brittany Staie, and Leroy Walston., *The 5 Cs of Agrivoltaic Success Factors in the United States: Lessons From the InSPIRE Research Study*, National Renewable Energy Laboratory, 2022.
- 9 S. Sanford, *Reducing greenhouse energy consumption— An overview*, University of Wisconsin-Extension, 2011.
- 10 E. Cuce, D. Harjunowibowo and P. M. Cuce, *Renewable and Sustainable Energy Reviews*, 2016, **64**, 34–59.
- 11 Agrivoltaics: Pairing Solar Power and Agriculture in the Northwest, <https://www.climatehubs.usda.gov/hubs/northwest/topic/agrivoltaics-pairing-solar-power-and-agriculture-northwest>, (accessed June 28, 2024).
- 12 Brite Solar – Solar Technologies, <https://www.britesolar.com>, (accessed July 29, 2024).
- 13 S. Sanford, *Reducing greenhouse energy consumption - An overview*, 2011.
- 14 R. H. EmamHassanien, *Renewable Energy*, 2018, **121**, 377–388.
- 15 A. M. Detweiler, C. E. Mioni, K. L. Hellier, J. J. Allen, S. A. Carter, B. M. Bebout, E. E. Fleming, C. Corrado and L. E. Prufert-Bebout, *Algal Research*, 2015, **9**, 170–177.
- 16 S. M. Lu, S. Amaducci, S. Gorjian, M. Haworth, C. Hägglund, T. Ma, S. Zainali and P. E. Campana, *Joule*, 2024, **8**, 2483–2522.
- 17 T. Warner, K. P. Ghigginio and G. Rosengarten, *Solar Energy*, 2022, **246**, 119–140.
- 18 O. Essahili, M. Ouafi and O. Moudam, *Solar Energy*, 2022, **245**, 58–66.
- 19 M. Kaltenbrunner, M. S. White, E. D. Głowacki, T. Sekitani, T. Someya, N. S. Sariciftci and S. Bauer, *Nat Commun*, 2012, **3**, 770.
- 20 C. J. M. Emmott, J. A. Röhr, M. Campoy-Quiles, T. Kirchartz, A. Urbina, N. J. Ekins-Daukes and J. Nelson, *Energy Environ. Sci.*, 2015, **8**, 1317–1328.
- 21 P. Cheng and Y. Yang, *Acc. Chem. Res.*, 2020, **53**, 1218–1228.
- 22 D. Meng, R. Zheng, Y. Zhao, E. Zhang, L. Dou and Y. Yang, *Advanced Materials*, 2022, **34**, 2107330.
- 23 N. Y. Doumon and L. J. A. Koster, *Solar RRL*, 2019, **3**, 1800301.
- 24 N. Y. Doumon, F. V. Houard, J. Dong, H. Yao, G. Portale, J. Hou and L. J. A. Koster, *Organic Electronics*, 2019, **69**, 255–262.
- 25 N. Y. Doumon, G. Wang, R. C. Chiechi, L. Jan and A. Koster, *J. Mater. Chem. C*, 2017, **5**, 6611.
- 26 M. Nam, H. Y. Noh, J.-H. Kang, J. Cho, B. K. Min, J. W. Shim and D.-H. Ko, *Nano Energy*, 2019, **58**, 652–659.



- 27 Y. Li, C. He, L. Zuo, F. Zhao, L. Zhan, X. Li, R. Xia, H.-L. Yip, C.-Z. Li, X. Liu and H. Chen, *Advanced Energy Materials*, 2021, **11**, 2003408.
- 28 W. Gao, Q. An, R. Ming, D. Xie, K. Wu, Z. Luo, Y. Zou, F. Zhang and C. Yang, *Advanced Functional Materials*, 2017, **1702194**, 1–10.
- 29 J. Hou, M. Park, S. Zhang, Y. Yao, L.-M. Chen, J.-H. Li and Y. Yang, *Macromolecules*, 2008, **41**, 6012–6018.
- 30 C. Zuo, H. J. Bolink, H. Han, J. Huang, D. Cahen and L. Ding, *Advanced Science*, 2016, **3**, 1500324.
- 31 J. Wang, Z. Zheng, P. Bi, Z. Chen, Y. Wang, X. Liu, S. Zhang, X. Hao, M. Zhang, Y. Li and J. Hou, *National Science Review*, 2023, **10**, nwad085.
- 32 Z. Zheng, J. Wang, P. Bi, J. Ren, Y. Wang, Y. Yang, X. Liu, S. Zhang and J. Hou, *Joule*, 2022, **6**, 171–184.
- 33 Z. Chen, J. Ge, W. Song, X. Tong, H. Liu, X. Yu, J. Li, J. Shi, L. Xie, C. Han, Q. Liu and Z. Ge, *Advanced Materials*, 2024, **36**, 2406690.
- 34 C. Liu, Y. Yang, H. Chen, J. Xu, A. Liu, A. S. R. Bati, H. Zhu, L. Grater, S. S. Hadke, C. Huang, V. K. Sangwan, T. Cai, D. Shin, L. X. Chen, M. C. Hersam, C. A. Mirkin, B. Chen, M. G. Kanatzidis and E. H. Sargent, *Science*, 2023, **382**, 810–815.
- 35 J. Park, J. Kim, H.-S. Yun, M. J. Paik, E. Noh, H. J. Mun, M. G. Kim, T. J. Shin and S. I. Seok, *Nature*, 2023, **616**, 724–730.
- 36 S.-H. Lim, H.-J. Seok, M.-J. Kwak, D.-H. Choi, S.-K. Kim, D.-H. Kim and H.-K. Kim, *Nano Energy*, 2021, **82**, 105703.
- 37 Y. Zhu, L. Shu and Z. Fan, *Chem. Res. Chin. Univ.*, 2020, **36**, 366–376.
- 38 J. Sun and J. J. Jasieniak, *J. Phys. D: Appl. Phys.*, 2017, **50**, 093001.
- 39 H. Lee, S. Jeong, J.-H. Kim, Y.-R. Jo, H. J. Eun, B. Park, S. C. Yoon, J. H. Kim, S.-H. Lee and S. Park, *npj Flex Electron*, 2023, **7**, 1–9.
- 40 O. Kruse, J. Rupprecht, J. H. Mussnug, G. C. Dismukes and B. Hankamer, *Photochem Photobiol Sci*, 2005, **4**, 957–970.
- 41 E. J. Stallknecht, C. K. Herrera, C. Yang, I. King, T. D. Sharkey, R. R. Lunt and E. S. Runkle, *Sci Rep*, 2023, **13**, 1903.
- 42 H.-W. Cheng, Y. Zhao and Y. Yang, *Advanced Energy Materials*, 2022, **12**, 2102908.
- 43 R. E. Blankenship, *Molecular Mechanisms of Photosynthesis*, John Wiley & Sons, 2021.
- 44 X.-G. Zhu, S. P. Long and D. R. Ort, *Curr Opin Biotechnol*, 2008, **19**, 153–159.
- 45 L. La Notte, L. Giordano, E. Calabrò, R. Bedini, G. Colla, G. Puglisi and A. Reale, *Applied Energy*, 2020, **278**, 115582.
- 46 R. Waller, M. Kacira, E. Magadley, M. Teitel and I. Yehia, *Agronomy*, 2021, **11**, 1152.
- 47 C. J. Traverse, R. Pandey, M. C. Barr and R. R. Lunt, *Nat Energy*, 2017, **2**, 849–860.
- 48 K. J. McCree, *Agricultural Meteorology*, 1971, **9**, 191–216.
- 49 H. Shi, L. Zhang, H. Huang, X. Wang, Z. Li, D. Xuan, C. Wang, Y. Ou, C. Ni, D. Li, D. Chi and S. Huang, *Small*, 2022, **18**, 2202144.
- 50 Z. Yuan, M. Zhang, Z. Yen, M. Feng, X. Jin, A. Ibrahim, M. G. Ahmed, T. Salim, R. A. Gonçalves, T. C. Sum, Y. M. Lam and L. H. Wong, *ACS Appl. Mater. Interfaces*, 2023, **15**, 37629–37639.



- 51 E. Kondolot Solak and E. Irmak, *RSC Advances*, 2023, **13**, 12244–12269.
- 52 K. N'Konou, S. Y. Kim and N. Y. Doumon, *Carbon Energy*, 2024, e579.
- 53 F. Machui, M. Hösel, N. Li, G. D. Spyropoulos, T. Ameri, R. R. Søndergaard, M. Jørgensen, A. Scheel, D. Gaiser, K. Kreul, D. Lenssen, M. Legros, N. Lemaitre, M. Vilkmann, M. Välimäki, S. Nordman, C. J. Brabec and F. C. Krebs, *Energy Environ. Sci.*, 2014, **7**, 2792–2802.
- 54 C.-S. Tsao, C.-M. Chuang, H.-C. Cha, Y.-Y. Huang, Y.-M. Sung, T.-Y. Chung, Y.-T. Chang, Z.-C. Hu, T.-C. Liu, W.-Y. Ma, Y.-H. Wang, K.-P. Chang, Y.-C. Chao and H.-F. Meng, *Materials Today Energy*, 2023, **36**, 101340.
- 55 X. Ru, M. Yang, S. Yin, Y. Wang, C. Hong, F. Peng, Y. Yuan, C. Sun, C. Xue, M. Qu, J. Wang, J. Lu, L. Fang, H. Deng, T. Xie, S. (Frank) Liu, Z. Li and X. Xu, *Joule*, 2024, **8**, 1092–1104.
- 56 A. M. Oni, A. S. M. Mohsin, Md. M. Rahman and M. B. Hossain Bhuiyan, *Energy Reports*, 2024, **11**, 3345–3366.
- 57 X. Liu, B. P. Rand and S. R. Forrest, *TRECHEM*, 2019, **1**, 815–829.
- 58 S. Rafique, S. M. Abdullah, K. Sulaiman and M. Iwamoto, *Renewable and Sustainable Energy Reviews*, 2017, **84**, 43–53.
- 59 E. A. Milani, M. Piralaee, S. Ahmadi and A. Asgari, *Sci Rep*, 2022, **12**, 14928.
- 60 S. Cook, H. Ohkita, Y. Kim, J. J. Benson-Smith, D. D. C. Bradley and J. R. Durrant, *Chemical Physics Letters*, 2007, **445**, 276–280.
- 61 S.-H. Liao, H.-J. Jhuo, Y.-S. Cheng and S.-A. Chen, *Advanced Materials*, 2013, **25**, 4766–4771.
- 62 Y. Lin, J. Wang, Z.-G. Zhang, H. Bai, Y. Li, D. Zhu and X. Zhan, *Adv Mater*, 2015, **27**, 1170–1174.
- 63 C. J. Brabec, F. Padinger, J. C. Hummelen, R. A. J. Janssen and N. S. Sariciftci, *Synthetic Metals*, 1999, **102**, 861–864.
- 64 K. Liu, Y. Jiang, G. Ran, F. Liu, W. Zhang and X. Zhu, *Joule*, 2024, **8**, 835–851.
- 65 Y.-W. Su, C.-E. Tsai, T.-C. Liao and K.-H. Wei, *Solar RRL*, 2024, **8**, 2300927.
- 66 Z. Wu, H. Yin, G. Li and Z. Ji, *Organic Electronics*, 2024, **129**, 107060.
- 67 B. Jia, S. Dai, Z. Ke, C. Yan, W. Ma and X. Zhan, *Chem. Mater.*, 2018, **30**, 239–245.
- 68 W. Wang, C. Yan, T.-K. Lau, J. Wang, K. Liu, Y. Fan, X. Lu and X. Zhan, *Advanced Materials*, 2017, **29**, 1701308.
- 69 J. Yuan, Y. Zhang, L. Zhou, G. Zhang, H.-L. Yip, T.-K. Lau, X. Lu, C. Zhu, H. Peng, P. A. Johnson, M. Leclerc, Y. Cao, J. Ulanski, Y. Li and Y. Zou, *Joule*, 2019, **3**, 1140–1151.
- 70 Y. Liu, P. Cheng, T. Li, R. Wang, Y. Li, S.-Y. Chang, Y. Zhu, H.-W. Cheng, K.-H. Wei, X. Zhan, B. Sun and Y. Yang, *ACS Nano*, 2019, **13**, 1071–1077.
- 71 Y. Li, X. Guo, Z. Peng, B. Qu, H. Yan, H. Ade, M. Zhang and S. R. Forrest, *Proceedings of the National Academy of Sciences*, 2020, **117**, 21147–21154.
- 72 Y. Bai, C. Zhao, X. Chen, S. Zhang, S. Zhang, T. Hayat, A. Alsaedi, Z. Tan, J. Hou and Y. Li, *J. Mater. Chem. A*, 2019, **7**, 15887–15894.
- 73 H. I. Jeong, S. Biswas, S. C. Yoon, S.-J. Ko, H. Kim and H. Choi, *Advanced Energy Materials*, 2021, **11**, 2102397.



- 74 Y. Zhao, P. Cheng, H. Yang, M. Wang, D. Meng, Y. Zhu, R. Zheng, T. Li, A. Zhang, S. Tan, T. Huang, J. Bian, X. Zhan, P. S. Weiss and Y. Yang, *ACS Nano*, 2022, **16**, 1231–1238.
- 75 B. Chang, Y.-C. Lin, S. Tan, C.-H. Chen, H.-W. Cheng, Y. Zhao, H.-C. Wang, Q. Xing, L.-Y. Chen, C.-A. Hsieh, C.-Y. Hsiao, Y. Yang and K.-H. Wei, *ACS Appl. Energy Mater.*, 2022, **5**, 13763–13772.
- 76 C. Xu, K. Jin, Z. Xiao, Z. Zhao, Y. Yan, X. Zhu, X. Li, Z. Zhou, S. Y. Jeong, L. Ding, H. Y. Woo, G. Yuan and F. Zhang, *Solar RRL*, 2022, **6**, 2200308.
- 77 X. Liu, Z. Zhong, R. Zhu, J. Yu and G. Li, *Joule*, 2022, **6**, 1918–1930.
- 78 S. Guan, Y. Li, K. Yan, W. Fu, L. Zuo and H. Chen, *Advanced Materials*, 2022, **34**, 2205844.
- 79 M. A. Sandri, J. L. Andriolo, M. Witter and T. Dal Ross, *Hortic. Bras.*, 2003, **21**, 642–645.
- 80 J. Jing, S. Dong, K. Zhang, Z. Zhou, Q. Xue, Y. Song, Z. Du, M. Ren and F. Huang, *Advanced Energy Materials*, 2022, **12**, 2200453.
- 81 M. Yan, P. J. Skabara and H. Meng, *J. Mater. Chem. C*, 2023, **11**, 8480–8485.
- 82 M. F. Albab, M. Jahandar, Y. H. Kim, Y.-K. Kim, M. Shin, A. Prasetio, S. Kim and D. C. Lim, *Nano Energy*, 2024, **121**, 109219.
- 83 A. Kojima, K. Teshima, Y. Shirai and T. Miyasaka, *Journal of the American Chemical Society*, 2009, **131**, 6050–6051.
- 84 Z.-R. Lan, Y.-D. Wang, J.-Y. Shao, D.-X. Ma, Z. Liu, D. Li, Y. Hou, J. Yao and Y.-W. Zhong, *Advanced Functional Materials*, 2024, **34**, 2312426.
- 85 Q. Dong, Y. Fang, Y. Shao, P. Mulligan, J. Qiu, L. Cao and J. Huang, *Science*, 2015, **347**, 967–970.
- 86 S. De Wolf, J. Holovsky, S.-J. Moon, P. Löper, B. Niesen, M. Ledinsky, F.-J. Haug, J.-H. Yum and C. Ballif, *J. Phys. Chem. Lett.*, 2014, **5**, 1035–1039.
- 87 Y. Zhao, A. M. Nardes and K. Zhu, *J. Phys. Chem. Lett.*, 2014, **5**, 490–494.
- 88 J. J. Yoo, G. Seo, M. R. Chua, T. G. Park, Y. Lu, F. Rotermund, Y.-K. Kim, C. S. Moon, N. J. Jeon, J.-P. Correa-Baena, V. Bulović, S. S. Shin, M. G. Bawendi and J. Seo, *Nature*, 2021, **590**, 587–593.
- 89 J. Jeong, M. Kim, J. Seo, H. Lu, P. Ahlawat, A. Mishra, Y. Yang, M. A. Hope, F. T. Eickemeyer, M. Kim, Y. J. Yoon, I. W. Choi, B. P. Darwich, S. J. Choi, Y. Jo, J. H. Lee, B. Walker, S. M. Zakeeruddin, L. Emsley, U. Rothlisberger, A. Hagfeldt, D. S. Kim, M. Grätzel and J. Y. Kim, *Nature*, 2021, **592**, 381–385.
- 90 I. M. Asuo, D. Gedamu, N. Y. Doumon, I. Ka, A. Pignolet, S. G. Cloutier and R. Nechache, *Materials Advances*, 2020, **1**, 1866–1876.
- 91 I. M. Asuo, I. Ka, D. Gedamu, A. Pignolet, R. Nechache and S. G. Cloutier, *Solar Energy Materials and Solar Cells*, 2019, **200**, 110029.
- 92 I. M. Asuo, A. M. Varposhti, E. D. Gomez and N. Y. Doumon, *J. Mater. Chem. C*, 2024, **12**, 7562–7571.
- 93 M. A. Green, A. Ho-Baillie and H. J. Snaith, *Nature Photon*, 2014, **8**, 506–514.
- 94 S. Tao, I. Schmidt, G. Brocks, J. Jiang, I. Tranca, K. Meerholz and S. Olthof, *Nat Commun*, 2019, **10**, 2560.
- 95 J. C. Yu, B. Li, C. J. Dunn, J. Yan, B. T. Diroll, A. S. R. Chesman and J. J. Jasieniak, *Advanced Science*, 2022, **9**, 2201487.



- 96 D. B. Ritzer, B. A. Nejand, M. A. Ruiz-Preciado, S. Gharibzadeh, H. Hu, A. Diercks, T. Feeney, B. S. Richards, T. Abzieher and U. W. Paetzold, *Energy Environ. Sci.*, 2023, **16**, 2212–2225.
- 97 E. Dănilă and D. D. Lucache, in *2016 International Conference and Exposition on Electrical and Power Engineering (EPE)*, 2016, pp. 439–444.
- 98 A. Trivellini, S. Toscano, D. Romano and A. Ferrante, *Plants (Basel)*, 2023, **12**, 2026.
- 99 K. M. Folta and S. A. Maruhnich, *Journal of Experimental Botany*, 2007, **58**, 3099–3111.
- 100 X. Rodríguez-Martínez, S. Riera-Galindo, L. E. Aguirre, M. Campoy-Quiles, H. Arwin and O. Inganäs, *Advanced Functional Materials*, 2023, **33**, 2213220.
- 101 T. Ma, S. Wang, Y. Zhang, K. Zhang and L. Yi, *J Mater Sci*, 2020, **55**, 464–479.
- 102 How are LEDs used for growing plants?, <https://www.circuitbread.com/ee-faq/how-are-leds-used-for-growing-plants>, (accessed July 3, 2024).
- 103 Y. (Michael) Yang, W. Chen, L. Dou, W.-H. Chang, H.-S. Duan, B. Bob, G. Li and Y. Yang, *Nature Photon*, 2015, **9**, 190–198.
- 104 R. Yu, H. Yao and J. Hou, *Advanced Energy Materials*, 2018, **8**, 1702814.
- 105 B. B. Lin, *Agricultural and Forest Meteorology*, 2010, **150**, 510–518.
- 106 H. A. Ahemd, A. A. Al-Faraj and A. M. Abdel-Ghany, *Scientia Horticulturae*, 2016, **201**, 36–45.
- 107 M. Möller and S. Assouline, *Irrig Sci*, 2007, **25**, 171–181.
- 108 R. H. E. Hassanien, M. Li and F. Yin, *Renewable Energy*, 2018, **121**, 377–388.
- 109 G. K. Ntinis, K. Kadoglidou, N. Tsivelika, K. Krommydas, A. Kalivas, P. Ralli and M. Irakli, *Horticulturae*, 2019, **5**, 42.
- 110 M. Cossu, A. Yano, S. Solinas, P. A. Deligios, M. T. Tiloca, A. Cossu and L. Ledda, *European Journal of Agronomy*, 2020, **118**, 126074.
- 111 M. A. Sandri, J. L. Andriolo, M. Witter and T. Dal Ross, *Hortic. Bras.*, 2003, **21**, 642–645.
- 112 J. D. Stamford, J. Stevens, P. M. Mullineaux and T. Lawson, 2023, **52**, 180–196.
- 113 M. Teitel, R. Grimberg, S. Ozer, H. Vitoshkin, I. Yehia, E. Magadley, A. Levi, E. Ziffer, S. Gantz and A. Levy, *Biosystems Engineering*, 2023, **232**, 81–96.
- 114 M. Friman-Peretz, S. Ozer, F. Geoola, E. Magadley, I. Yehia, A. Levi, R. Brikman, S. Gantz, A. Levy, M. Kacira and M. Teitel, *Biosystems Engineering*, 2020, **197**, 12–31.
- 115 M. Friman Peretz, F. Geoola, I. Yehia, S. Ozer, A. Levi, E. Magadley, R. Brikman, L. Rosenfeld, A. Levy, M. Kacira and M. Teitel, *Biosystems Engineering*, 2019, **184**, 24–36.
- 116 N. Gnayem, E. Magadley, A. Haj-Yahya, S. Masalha, R. Kabha, A. Abasi, H. Barhom, M. Matar, M. Attrash and I. Yehia, *Biosystems Engineering*, 2024, **241**, 83–94.
- 117 K. Okada, I. Yehia, M. Teitel and M. Kacira, *Acta Horticulturae*, 2018, **1227**, 231–239.
- 118 R. Waller, M. Kacira, E. Magadley, M. Teitel and I. Yehia, *AgriEngineering*, 2022, **4**, 969–992.
- 119 S. Y. Kim, C. C. F. Kumachang and N. Y. Doumon, *Solar RRL*, 2023, **7**, 2300155.



- 120 Y. Zhao, Z. Li, C. Deger, M. Wang, M. Peric, Y. Yin, D. Meng, W. Yang, X. Wang, Q. Xing, B. Chang, E. G. Scott, Y. Zhou, E. Zhang, R. Zheng, J. Bian, Y. Shi, I. Yavuz, K.-H. Wei, K. N. Houk and Y. Yang, *Nat Sustain*, 2023, **6**, 539–548.
- 121 L. Duan and A. Uddin, *Advanced Science (Weinheim, Baden-Wuerttemberg, Germany)*, 2020, **7**, 1903259.
- 122 C. J. Schaffer, C. M. Palumbiny, M. A. Niedermeier, C. Jendrzewski, G. Santoro, S. V. Roth and P. Müller-Buschbaum, *Adv Mater*, 2013, **25**, 6760–6764.
- 123 A. Turak, *RSC Advances*, 2013, **3**, 6188–6225.
- 124 D. Wang, M. Wright, N. K. Elumalai and A. Uddin, *Solar Energy Materials and Solar Cells*, 2016, **147**, 255–275.
- 125 D. C. Lim, J. H. Jeong, K. Hong, S. Nho, J.-Y. Lee, Q. V. Hoang, S. K. Lee, K. Pyo, D. Lee and S. Cho, *Progress in Photovoltaics: Research and Applications*, 2018, **26**, 188–195.
- 126 L. Sun, W. Zeng, C. Xie, L. Hu, X. Dong, F. Qin, W. Wang, T. Liu, X. Jiang, Y. Jiang and Y. Zhou, *Advanced Materials*, 2020, **32**, 1907840.
- 127 D.-S. Leem, A. Edwards, M. Faist, J. Nelson, D. D. C. Bradley and J. C. de Mello, *Advanced Materials*, 2011, **23**, 4371–4375.
- 128 A. Kim, Y. Won, K. Woo, S. Jeong and J. Moon, *Advanced Functional Materials*, 2014, **24**, 2462–2471.
- 129 S. Lee, D. Jeong, C. Kim, C. Lee, H. Kang, H. Y. Woo and B. J. Kim, *ACS Nano*, 2020, **14**, 14493–14527.
- 130 F. Campana, C. Kim, A. Marrocchi and L. Vaccaro, *Journal of Materials Chemistry C*, 2020, **8**, 15027–15047.
- 131 Y.-T. Huang, S. R. Kavanagh, D. O. Scanlon, A. Walsh and R. L. Z. Hoyer, *Nanotechnology*, 2021, **32**, 132004.
- 132 A. Babayigit, A. Ethirajan, M. Muller and B. Conings, *Nature Mater*, 2016, **15**, 247–251.
- 133 D. Yan, X. Lu, S. Zhao, Z. Zhang, M. Lu, J. Feng, J. Zhang, K. Spencer, T. Watson, M. Li, B. Hou, F. Wang and Z. Li, *Solar RRL*, 2022, **6**, 2200332.
- 134 F. Gu, Z. Zhao, C. Wang, H. Rao, B. Zhao, Z. Liu, Z. Bian and C. Huang, *Solar RRL*, 2019, **3**, 1900213.
- 135 L. Gollino and T. Pauporté, *Solar RRL*, 2021, **5**, 2000616.
- 136 L. Wang, M. Chen, S. Yang, N. Uezono, Q. Miao, G. Kapil, A. K. Baranwal, Y. Sanehira, D. Wang, D. Liu, T. Ma, K. Ozawa, T. Sakurai, Z. Zhang, Q. Shen and S. Hayase, *ACS Energy Lett.*, 2022, **7**, 3703–3708.
- 137 L. Wang, Q. Miao, D. Wang, M. Chen, H. Bi, J. Liu, A. K. Baranwal, G. Kapil, Y. Sanehira, T. Kitamura, T. Ma, Z. Zhang, Q. Shen and S. Hayase, *Angewandte Chemie International Edition*, 2023, **62**, e202307228.
- 138 A. Mei, Y. Sheng, Y. Ming, Y. Hu, Y. Rong, W. Zhang, S. Luo, G. Na, C. Tian, X. Hou, Y. Xiong, Z. Zhang, S. Liu, S. Uchida, T.-W. Kim, Y. Yuan, L. Zhang, Y. Zhou and H. Han, *Joule*, 2020, **4**, 2646–2660.
- 139 M. L. Rencheck, C. Libby, A. Montgomery and J. S. Stein, *Solar Energy*, 2024, **269**, 112337.
- 140 X. Li, F. Zhang, H. He, J. J. Berry, K. Zhu and T. Xu, *Nature*, 2020, **578**, 555–558.



- 141 G. Liu, Y. Zhong, W. Feng, M. Yang, G. Yang, J.-X. Zhong, T. Tian, J.-B. Luo, J. Tao, S. Yang, X.-D. Wang, L. Tan, Y. Chen and W.-Q. Wu, *Angewandte Chemie International Edition*, 2022, **61**, e202209464.
- 142 C. Fei, N. Li, M. Wang, X. Wang, H. Gu, B. Chen, Z. Zhang, Z. Ni, H. Jiao, W. Xu, Z. Shi, Y. Yan and J. Huang, *Science*, 2023, **380**, 823–829.
- 143 H. Zhang, J.-W. Lee, G. Nasti, R. Handy, A. Abate, M. Grätzel and N.-G. Park, *Nature*, 2023, **617**, 687–695.
- 144 Y.-M. Li, Y. Wang, M.-J. Chen, T.-Y. Huang, F.-H. Yang and Z.-J. Wang, *Int. J. Environ. Sci. Technol.*, 2023, **20**, 1037–1052.
- 145 M. S. Rahmanifar, *Electrochimica Acta*, 2017, **235**, 10–18.
- 146 U. N. Environment, Used Lead Acid Batteries (ULAB) - Waste Lead Acid Batteries (WLAB), <http://www.unep.org/topics/chemicals-and-pollution-action/pollution-and-health/heavy-metals/used-lead-acid-batteries>, (accessed July 15, 2024).
- 147 B. Chen, C. Fei, S. Chen, H. Gu, X. Xiao and J. Huang, *Nat Commun*, 2021, **12**, 5859.
- 148 L. Shen and X. Yin, *Nano Convergence*, 2022, **9**, 36.
- 149 Heliatek achieves ICE 61215 certification for lightweight and flexible HeliaSol solar film, <https://ope-journal.com/news/heliatek-achieves-ice-61215-certification-for-lightweight-and-flexible-heliasol-solar-film>, (accessed July 15, 2024).
- 150 L. Shi, T. L. Young, J. Kim, Y. Sheng, L. Wang, Y. Chen, Z. Feng, M. J. Keevers, X. Hao, P. J. Verlinden, M. A. Green and A. W. Y. Ho-Baillie, *ACS Appl. Mater. Interfaces*, 2017, **9**, 25073–25081.
- 151 L. Shi, M. P. Bucknall, T. L. Young, M. Zhang, L. Hu, J. Bing, D. S. Lee, J. Kim, T. Wu, N. Takamure, D. R. McKenzie, S. Huang, M. A. Green and A. W. Y. Ho-Baillie, *Science*, 2020, **368**, eaba2412.
- 152 A. Mei, Y. Sheng, Y. Ming, Y. Hu, Y. Rong, W. Zhang, S. Luo, G. Na, C. Tian, X. Hou, Y. Xiong, Z. Zhang, S. Liu, S. Uchida, T.-W. Kim, Y. Yuan, L. Zhang, Y. Zhou and H. Han, *Joule*, 2020, **4**, 2646–2660.
- 153 L. Zhang, Y. Wang, X. Meng, J. Zhang, P. Wu, M. Wang, F. Cao, C. Chen, Z. Wang, F. Yang, X. Li, Y. Zou, X. Jin, Y. Jiang, H. Li, Y. Liu, T. Bu, B. Yan, Y. Li, J. Fang, L. Xiao, J. Yang, F. Huang, S. Liu, J. Yao, L. Liao, L. Li, F. Zhang, Y. Zhan, Y. Chen, Y. Mai and L. Ding, *Mater. Futures*, 2024, **3**, 022101.
- 154 Agrivoltaics Map, https://openei.org/wiki/InSPIRE/Agrivoltaics_Map, (accessed July 15, 2024).



**PennState****Nutifafa Y. Doumon, Ph.D., MA**Assistant Professor
Virginia S. and Philip L. Walker Jr. Faculty Fellow
Materials Science and Engineering
The Pennsylvania State University
333 Steidle Building
University Park, PA 16802nzd5349@psu.edu
doumonlab-semde.matse.psu.edu

Data Availability Statement

Data sharing is not applicable to this article as no datasets were generated or analysed for the current manuscript.

On behalf of all co-authors

Nutifafa Y. Doumon, PhD, MA

Virginia S. and Philip L. Walker Jr. Professor of Materials Science and Engineering

